SKILL COMPARISON OF SOME DYNAMICAL AND EMPIRICAL DOWNSCALING METHODS FOR SOUTHERN AFRICA FROM A SEASONAL CLIMATE MODELLING PERSPECTIVE

by

WILLEM A. LANDMAN, MARY-JANE KGATUKE, MALUTA MBEDZI,
ASMEROM BERAKI, ANNA BARTMAN, ANNELISE DU PIESANIE

South African Weather Service

Report to the Water Research Commission

Report No 1334/1/06
ISBN No: 1-77005-470-7

2006

EXECUTIVE SUMMARY

1. Introduction and Objectives

The main emphasis of the project was to assess the ability of an advanced state-of-the-art, albeit computationally expensive, method of downscaling large-scale climate predictions to regional and local scale as a seasonal rainfall forecasting tool for southern Africa in order to improve seasonal outlook information for hydrological purposes. Downscaling the large scale to more localized seasonal rainfall over southern Africa had been shown to be feasible, but further research in downscaling, with both improved spatial and temporal resolution, was required. The main aims of the project were to:

1. Set base-line forecast skill levels, using statistical models;
2. Compile an appropriate general circulation model (GCM) climatology of a sufficiently large ensemble;
3. Nest dynamical regional climate models in the GCM simulated large scale fields;
4. Compare the nested scheme's forecast skill with the base-line skill levels.

2. Results and Conclusions

Ultimately, various downscaling techniques and raw GCM output were compared to one another over the 10-year period from 1991/92 to 2000/01 and also to a baseline prediction technique that uses only global sea-surface temperature (SST) anomalies as predictors. The various downscaling techniques described in this study include both an empirical technique called model output statistics (MOS) and a dynamical technique where a finer resolution regional climate model (RCM) was nested into the large-scale fields of a coarser GCM. The study concluded by investigating the internal variability of the RCM.

The study addressed the performance of a number of simulation systems (no forecast lead-time) of varying complexity. These systems' performance was tested for the December-January-February (DJF) rainfall for both homogeneous regions and for 963 stations over South Africa, and compared with each other over a 10-year test period from 1991/92 to 2000/01. For the most part the simulation methods outscored the baseline method that used sea-surface temperature (SST) anomalies to simulate rainfall, thereby providing evidence that current approaches in seasonal forecasting are outscoring earlier ones. Current operational forecasting approaches involve the use of GCMs which are considered to be the main tool whereby seasonal forecasting efforts will improve in the future. Moreover, advantages in statistically post-processing output from GCMs as well as output from regional climate models (RCMs) were demonstrated. Skill should further improve with an increased number of ensemble members. However, multiple realizations are not required to describe the internal variability of the nested system, which suggests that increasing the ensemble size would mainly contribute to probabilistic forecast skill.

3. Recommendations

The potential for using dynamical and statistical downscaling methods and their combination for modelling South African seasonal regional rainfall variability was demonstrated. In addition to expanding on the number of ensemble members, the test period of 10 years should be increased in order to test the robustness of the results presented here since this test period may be too short to unequivocally demonstrate which simulation method is the best. An increased ensemble size can also be considered to test the probabilistic skill levels of these systems and how they can be used in an operational seasonal forecasting environment that demands a description of forecast uncertainties.

REPORT ON CAPACITY BUILDING

1. Workshops

1.1. Local workshop

A regional atmospheric modelling workshop, sponsored by the WRC, was presented during the week of 25-29 November 2002. The workshop was co-presented by the South African Weather Service (SAWS) and the University of Pretoria, and focused on the physical parameterization schemes of regional models, with specific emphasis on cumulus parameterization schemes. The regional models that were tested are research models such as the DARLAM and MM5. The invited guest was Dr Anji Seth who specializes in regional climate modelling and is a research scientist from the International Research Institute for Climate and Society (IRI) in New York. Delegates from nine SADC countries attended. The countries were Namibia, Zambia, Tanzania, Botswana, Zimbabwe, Mauritius, Lesotho, Swaziland and South Africa.

1.2. International workshop

Mary-Jane Kgatuke was supported by WRC research funds to attend a regional climate modelling workshop in Trieste, Italy. The workshop was intended to provide lectures and extensive hands-on sessions on the theory of regional climate change and regional climate modelling systems. The new version of the regional climate model, the RegCM3, was released. The participants obtained skill in installing and running the new version of the regional climate model. The RegCM3 was subsequently installed at the SAWS and formed an integral part of the project K5/1334.

2. Post-graduate research

Mary-Jane Kgatuke completed an MSc research project on the internal variability of the RegCM3. The dissertation has been submitted for examination as part of the requirement for the degree of MSc(Meteorology) at the University of Pretoria.

3. Training on the Regional Spectral Model (RSM)

Annelise du Piesanie and Maluta Mbedzi received training at the IRI on the RSM and the model has subsequently been installed at the SAWS. This model is planned to be part of the multi regional model ensemble to be run operationally at the SAWS.

ARCHIVING OF DATA

The RegCM3 10-year climatology will be used by the SAWS to make operational fine resolution forecasts for December-February seasons, starting in November 2006. The SAWS will maintain the archived data and also make a backup archive. The RegCM3 data are available for any academic institution for research purposes. To get access to these data sets, contact Maluta Mbedzi at the SAWS (tel: 012-367-6243, email: maluta@weathersa.co.za).

KNOWLEDGE DISSEMINATION

1. Ms Mary-Jane Kgatuke completed an MSc dissertation entitled "Internal variability of the regional climate model RegCM3 over southern Africa", at the University of Pretoria.
2. The following papers are based on the results presented in the report:
   a. Internal variability of the RegCM3 over South Africa, by M. M. Kgatuke, W. A. Landman, A. Beraki and M. Mbedzi. Submitted to the *International Journal of Climatology*.
   b. Skill comparisons of some dynamical and empirical downscaling methods for South Africa from a seasonal climate modelling perspective, by W. A. Landman, M. M. Kgatuke, M. Mbedzi, A. Beraki, A. Bartman and A. du Piesanie. In preparation for *Water SA*.
3. The following national conference presentation is a summary of the skill comparisons between the various methods:
   a. Skill comparisons of some dynamical and empirical downscaling methods for South Africa from a seasonal climate modelling perspective, by M. M. Kgatuke, W. A. Landman, M. Mbedzi, A. Beraki, A. Bartman and A. du Piesanie.

ACKNOWLEDGEMENTS

1. Dr. G. Green for his interest and support during the project.
2. Dr. L. Sun of the International Research Institute for Climate and Society (IRI) for making the ECHAM4.5 6-hourly data accessible.
3. Drs. S. Mason and L. Goddard of the IRI for suggestions to address the objectives of the project and for general discussions.
4. Dr. F. Giorgi for advising on the structure of the experiment on the internal variability of the RegCM3.
5. The authors also appreciate the comments of the Steering Committee: Dr G. Green, Mr R. Dube, Dr. M. Zunckel, Mr. E. Poolman, Prof. B. Hewitson, Prof. Johan van Heerden, Mr. B. du Plessis, Mr. S. Naidoo, and Prof. C. J. de W. Rautenbach.

TABLE OF CONTENTS

LIST OF FIGURES

Figure 3.3. Simulation skill (correlation) for each region using the 6 simulation methods. Horizontal lines indicate the 90% and 95% confidence levels. Asterisks show the 95% confidence intervals obtained from the Monte Carlo process.

Figure 3.4. Regional area-averaged simulation performances over the 10-year test period.

Figure 3.5. Regional area-average simulation performance of the raw ECHAM4.5-RegCM3 system and the ECHAM4.5-RegCM3-MOS system.

Figure 3.6. Regional area-average simulation performance of the ECHAM4.5-RegCM3 system and the NCEP-RegCM3 system.

Figure 4.1. Correlations between the ECHAM4.5-RegCM3 rainfall simulation (4-member mean) and the observed rainfall over the 10-year test period of 1991/92 to 2000/01. Correlation values less than 0 are masked out.

Figure 4.2. Correlations between the ECHAM4.5-MOS rainfall simulation (24-member mean) and the observed rainfall over the 10-year test period of 1991/92 to 2000/01. Correlation values less than 0 are masked out.

Figure 4.3. Correlations between the ECHAM4.5-MOS rainfall simulation (4-member mean) and the observed rainfall over the 10-year test period of 1991/92 to 2000/01. Correlation values less than 0 are masked out. The top panel shows the upper limit and the bottom panel the lower limit of the 95% significance level.

Figure 4.4. Correlations between the raw ECHAM4.5 rainfall simulation (24-member mean) and the observed rainfall over the 10-year test period of 1991/92 to 2000/01. Correlation values less than 0 are masked out.

Figure 4.5. Correlations between the raw ECHAM4.5 rainfall simulation (4-member mean) and the observed rainfall over the 10-year test period of 1991/92 to 2000/01. Correlation values less than 0 are masked out. The top panel shows the upper limit and the bottom panel the lower limit of the 95% significance level.

Figure 4.6. Correlations between the baseline model (using SSTs as predictor) and the observed rainfall over the 10-year test period of 1991/92 to 2000/01. Correlation values less than 0 are masked out.

Figure 4.7. Correlation differences between the ECHAM4.5-RegCM3 system and the ECHAM4.5-MOS system (full set ensemble of 24) over the 10-year test period of 1991/92 to 2000/01.

Figure 4.8. Correlation differences between the ECHAM4.5-RegCM3 system and the ECHAM4.5-MOS system (4 ensemble members) over the 10-year test period of 1991/92 to 2000/01. The top panel shows the upper limit and the bottom panel the lower limit of the 95% significance level.

Figure 4.9. Correlation differences between the ECHAM4.5-RegCM3 system and the raw ECHAM4.5 system (full set ensemble of 24) over the 10-year test period of 1991/92 to 2000/01.

Figure 4.10. Correlation differences between the ECHAM4.5-RegCM3 system and the raw ECHAM4.5 system (4 ensemble members) over the 10-year test period of 1991/92 to 2000/01. The top panel shows the upper limit and the bottom panel the lower limit of the 95% significance level.

Figure 4.11. Correlation differences between the ECHAM4.5-RegCM3 system and the baseline model (using SST to simulate rainfall) over the 10-year test period of 1991/92 to 2000/01.

Figure 4.12. Correlation differences between the ECHAM4.5-MOS and raw ECHAM4.5 systems (full ensemble of 24) over the 10-year test period of 1991/92 to 2000/01.

Figure 4.13. Correlation differences between the ECHAM4.5-MOS and raw ECHAM4.5 systems (4 ensemble members) over the 10-year test period of 1991/92 to 2000/01. The top panel shows the upper limit and the bottom panel the lower limit of the 95% significance level.

Figure 4.14. Correlation differences between the ECHAM4.5-MOS (full ensemble of 24) and the baseline system (SST as predictor) over the 10-year test period of 1991/92 to 2000/01.

Figure 4.15. Correlation differences between the ECHAM4.5-MOS (4 ensemble members) and the baseline model (SST as predictors) over the 10-year test period of 1991/92 to 2000/01. The top panel shows the upper limit and the bottom panel the lower limit of the 95% significance level.

Figure 4.16. Correlation differences between the raw ECHAM4.5 (full ensemble of 24) and the baseline system (SST as predictor) over the 10-year test period of 1991/92 to 2000/01.

Figure 4.17. Correlation differences between the raw ECHAM4.5 (4 ensemble members) and the baseline model (SST as predictors) over the 10-year test period of 1991/92 to 2000/01. The top panel shows the upper limit and the bottom panel the lower limit of the 95% significance level.

Figure 4.18. Regional area-averaged simulation performances over the 10-year test period.

LIST OF TABLES

CHAPTER 1:
INTRODUCTION

1.1. Background

Droughts and floods have long been distinctive features of the climate of southern Africa (Tyson and Preston-Whyte, 2000). Variability of the climate has been accentuated by the occurrence of the El Niño / Southern Oscillation (ENSO) phenomenon, but is by no means dominated by them (Mason and Jury, 1997). Climate variations have an important impact on agriculture, housing, water supply, industry and tourism. With an ever-increasing population that is putting an associated increase in demand on fresh water resources, effective water management has become essential. The need for providing improved seasonal rainfall forecasts, both temporally and spatially, is becoming more and more necessary in the region. Improvements to the prediction of southern Africa's summer rainfall on a seasonal scale will be best achieved using General Circulation Models (GCMs) (Landman et al. 2001a). Although GCMs, commonly configured with an effective resolution of 200-300 km, have demonstrated skill at global or even continental scale, they are unable to represent local sub-grid features, subsequently producing rainfall over southern Africa that is typically overestimated (Joubert and Hewitson, 1997; Mason and Joubert, 1997). Such systematic biases have created the need to downscale GCM simulations to regional level over southern Africa. Semi-empirical relationships exist between observed large-scale circulation and rainfall, and assuming that these relationships are valid under future climate conditions and also that the large-scale structure and variability is well characterized by GCMs, mathematical equations can be constructed to predict local precipitation from the simulated large-scale circulation (Wilby and Wigley, 1997). Empirical remapping of GCM fields to regional rainfall has been demonstrated successfully over southern

Africa (Landman and Goddard, 2002; Landman and Tennant, 2000; Landman et al. 2001a,b).

Further increase in resolution may be required over a specific area, which could be resolved by nesting a higher resolution limited area regional model within the global GCM (Giorgi, 1990). The nested model is run over a limited-area domain and is driven by time-dependent large-scale meteorological fields, such as output from a GCM. The nesting will improve on the topographic features that are poorly resolved by global models and the simulation of significant synoptic features inadequately simulated by coarser GCM resolutions. A finer resolution should thus improve on the understanding of how seasonal predictability is related to spatial scale, even though the choice of the regional model domain may have a significant impact on simulation results (Giorgi et al. 1996; Seth and Giorgi, 1998). However, given the most suitable domain, physical parameterizations and lower boundary conditions, a multi-year integration is required in order to properly recognize anomalous behaviour relative to the regional model's time-averaged behaviour (Goddard et al. 2001), which requires a large amount of computer time and storage space. Notwithstanding, nested modelling approaches are capable of simulating the details of regional climate over southern Africa with greater skill than global models (Joubert et al. 1999). The amount of variability in the nested system solutions that is introduced by an RCM's internal variability has to be analyzed to determine whether or not multiple realizations need to be generated in operational forecasting to quantify the uncertainty associated with the non-linearities in the RCM. Owing to the large expense involved when using a combination of GCMs and regional models and to a lesser extent a combination of GCMs and empirical downscaling methods, the GCM-based approaches to seasonal rainfall estimation should produce rainfall forecasts with skill that outscores that of simple empirical modelling, which may for example, utilize a linear relationship between oceanic and rainfall variability to assess the expected rainfall distribution of a coming season. The main objective is therefore to assess whether GCM-based approaches to seasonal rainfall estimation can produce rainfall forecasts with skill that outscores that of simple linear modelling. In addition, it is necessary to assess if the nested approach is more skilful than that of the computationally less expensive empirical downscaling approach.

1.2. Organization of the report

Chapter 1 gives an introduction to the need for and advances in seasonal forecasting in South Africa with special emphasis on downscaling. Chapter 2 is the description of the data used and simulation methods, including the descriptions of the GCM, RCM, GCM- and RCM-MOS and SST-forced statistical model. Optimal ensemble size of the GCM and ensemble spread are subsequently addressed. Also included is the selection of the optimal domain required for downscaling, and the regionalization of the rainfall stations into homogeneous regions. Simulation skill and skill differences between the various simulation techniques are described in Chapters 3 and 4. A study of the internal variability of the RCM is discussed in Chapter 5. Chapter 6 summarizes the research results, presents conclusions and key recommendations.

CHAPTER 2:

SIMULATION MODELS AND DATA PREPARATION

2.1. Observed rainfall data and homogenization

A total of 963 stations, more or less evenly distributed over South Africa, are used in the study (Figure 2.1). These stations are also grouped into regions where the stations within each region have the same interannual rainfall variability. Cluster analysis is used to group the stations into homogeneous rainfall regions based on the standardized monthly rainfall totals for the 45-year period of 1960 to 2004. The data are first standardized to eliminate problems of non-linearity that arise if the monthly rainfall totals do not have equal variance. It is evident that there are certain regions where the distribution of the stations is sparse, but knowledge of geographical and climatological characteristics are used to "extrapolate" the borders of some regions, introducing a small amount of subjectivity into the final definition of the borders of the region.

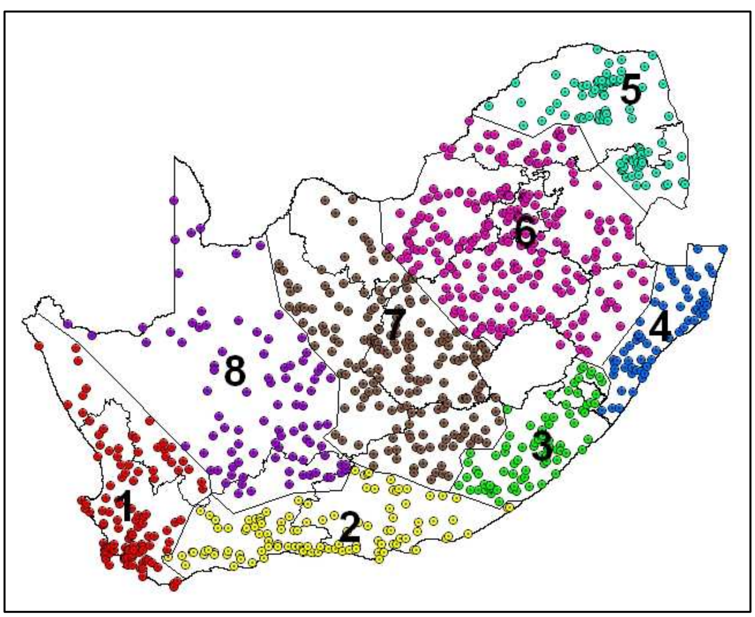

Figure 2.1. The eight homogeneous rainfall regions of South Africa. SAWS stations are shown as dots.

After the regionalization, monthly and 3-monthly indices are calculated for each region (Mason, 1998), using the raw monthly rainfall station data. Let x_{ijkp} represent the monthly or 3-monthly (seasonal) rainfall total for month or season *i*, year *j*, station *k* in region *p*. Then, for *m* stations in region *p*, the regional index z_{ijp} is calculated as follows:

$$z_{ijp} = \frac{1}{m}\sum_{p=1}^{m} \frac{x_{ijkp} - \bar{x}_{ikp}}{\sigma_{jkp}}$$

The regions, numbered in Figure 2.1, are named as follows:

Region 1: South-western Cape (SOWC); Region 2: South coast (SOUC); Region 3: Southern KwaZulu-Natal (SKZN); Region 4: Northern KwaZulu-Natal (NKZN); Region 5: Lowveld (LOWV); Region 6: Highveld (HIGH); Region 7: Central interior (CINT); and, Region 8: Western Interior.

2.2. The general circulation model

All GCM integrations were performed by the International Research Institute for Climate and Society (IRI) using the ECHAM4.5 AGCM (Roeckner et al, 1996). An ensemble of 24 runs was forced with simultaneous observed SSTs (SSTs occurring during the same season as the simulated rainfall season) (Reynolds and Smith, 1994; Smith et al., 1996) from 1950 to present. At initialization ensemble members differ from each other by one model day at the beginning of the integration. No observed atmospheric conditions are inserted into the runs at any time. The resulting AGCM fields are referred to as *simulation* mode fields (no forecast lead time). The GCM is successful in simulating the overall pattern of maximum rainfall over the north-east of South Africa decreasing towards the south-west, but it displaces slightly the local maximum over these regions and simulates lower rainfall totals than found in the observed climatology. Figure 2.2 shows associations between observed and GCM-simulated and observed and GCM-forecast rainfall fields for DJF as calculated over the period 1968 to 1997. Statistically significant correlations are found over southern Africa.

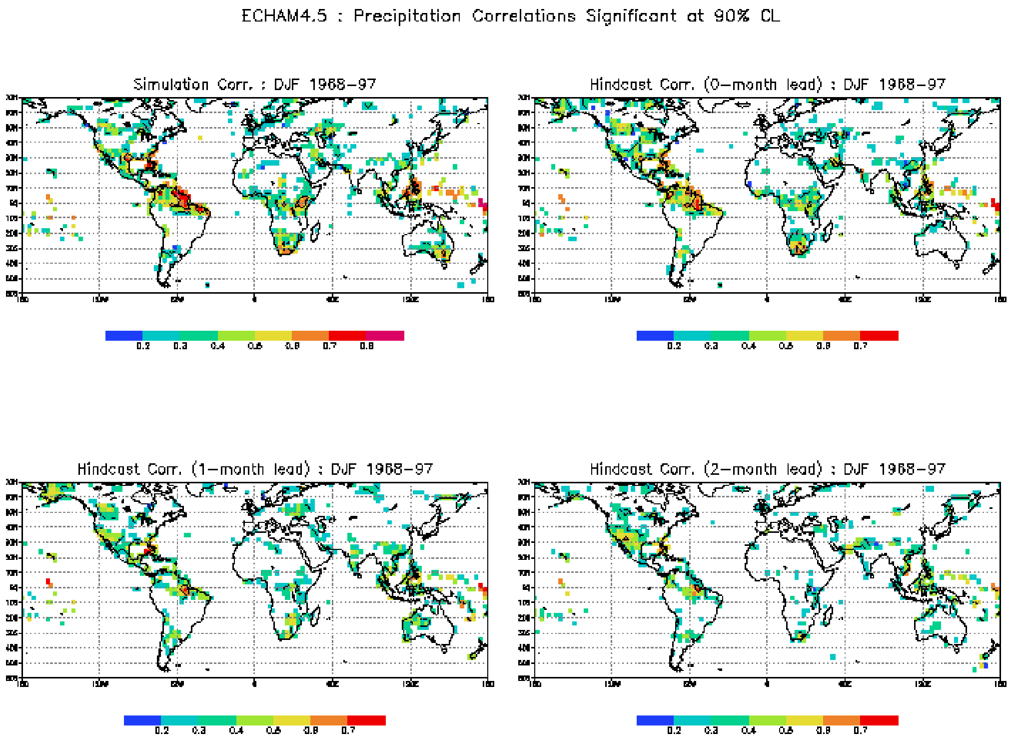

Figure 2.2. ECHAM4.5 skill for rainfall simulation and forecast runs.

While it is possible that an ensemble might show a reasonable degree of skill, that is to say the verification field lies within the range of the ensemble, another measure of the skill of the ensemble might be considered to be the (lack of) dispersion. Indeed the more widely dispersed the ensemble the more likely the chance of it's showing a degree of skill. At the same time the dispersion of the ensemble is indicative of the lack of skill of particular members and it is only in the ensemble treatment of the forecasts that skill is shown. It is well known that some form of averaging takes the best of each member and incorporates it into the mean.

The ensemble-skill is one aspect of the evaluation of the performance of the ensemble. Additionally it is important to consider the dispersion (of the skill) of individual forecasts within the ensemble. Also to be considered is the relationship between the dispersion of the skill and the dispersion of the forecasts. It is quite possible that the verification field lies within the range of the ensemble while at the same time the ensemble skill is low. There is a correlation between ensemble mean and the intra-ensemble dispersion of skill. However this correlation does not prove the existence of a relationship between ensemble dispersion and ensemble mean skill. Figure 2.3 shows the spread of the simulation mode ECHAM4.5 ensemble members (24) of the DJF simulated rainfall over the central interior of South Africa for the period 1988/89 to 1997/98.

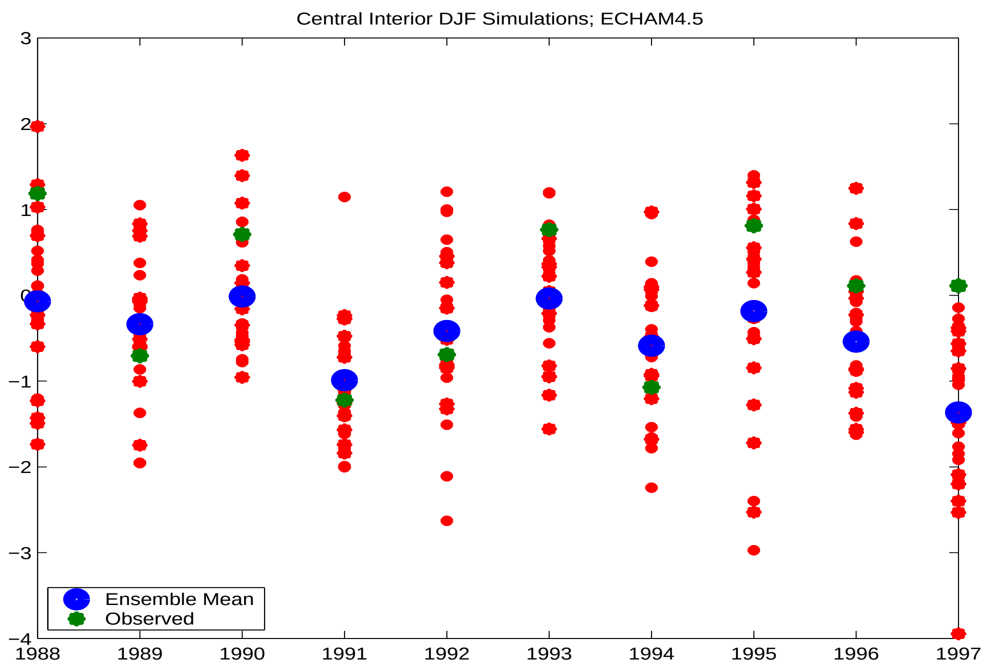

Figure 2.3. Central interior ECHAM4.5 DJF rainfall simulations. The red asterisks are the individual ensemble members, the green the observed and the blue the ensemble mean. Values have been standardized.

Figure 2.4 is the graph showing the percentage of model grid points exceeding a given anomaly correlation value for rainfall simulations compared to observations over southern Africa. 'r' is the correlation between the ensemble mean climate anomaly and the observed anomaly, at each model grid point, over the 1965/66 to 1997/98 period. For each case of fixed ensemble size, all the possible sub-sets of that number from the grand ensemble of 24 are considered. So for 3 ensemble members, all possible non-repetitive 3 from 24 are considered, i.e., (1 5 7), (2 3 17), etc. For 23 members, there would be 24 sub-sets with an increasing number of subsets for smaller ensemble size, but without any noticeable effect on the result. With a larger ensemble, the mean is better estimated, so the correlation is more stable. When the ensemble is smaller, there is more uncertainty in the correlation, but there are more sub-sets to average over and thus reduce the uncertainty.

The following example serves to explain the interpretation of Figure 2.4: There are no grid points with an ‘r’ greater than 0.7, and about 12% of the grid points have an ‘r’ greater than 0.5 for 16, 20 and 23 ensemble members. The figure shows that after about 16 ensemble members, improvements in simulating southern African DJF rainfall are only marginal. Therefore, the GCM simulation skill will not improve or deteriorate when the full set of 24 ensemble members are used in this study.

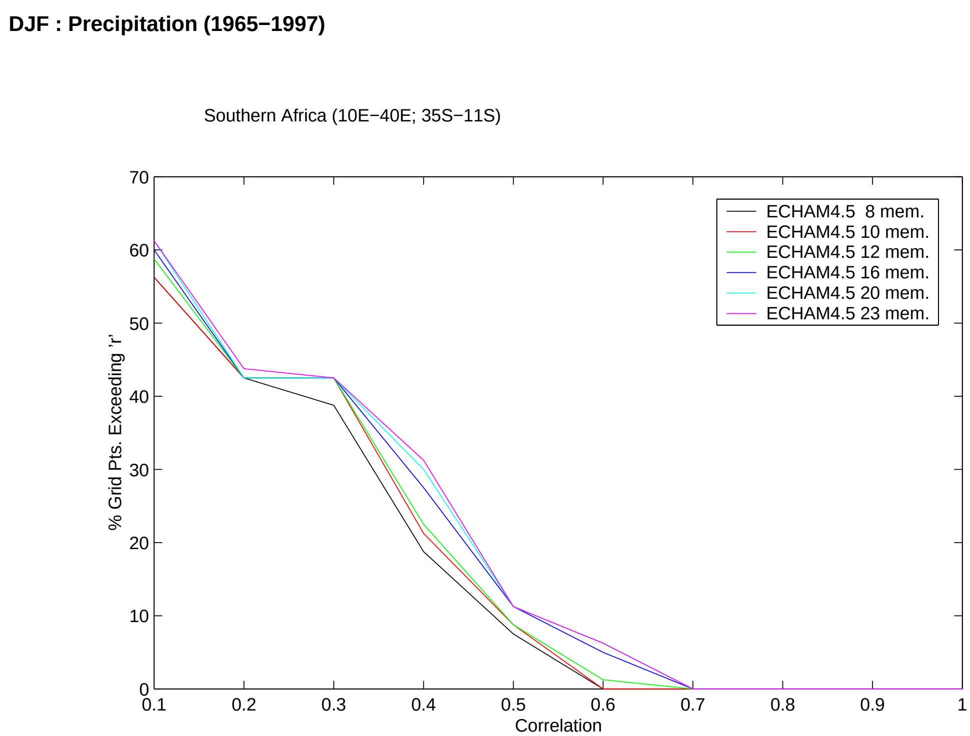

Figure 2.4. Graph showing the percentage of model grid points exceeding a given anomaly correlation value for rainfall simulations compared to observations over southern Africa (10E-40E; 35S-11S) during the DJF season, 1965-1997. Different line colours indicate different numbers of ensemble members, taken from a 24-member integration of the ECHAM4.5 atmospheric model, for which the ensemble mean was taken before comparison with observations. Note that the lines are plotted in order of increasing ensemble size.

2.3. The regional climate model

Dynamical downscaling utilizes high resolution regional climate models (RCMs) to derive regional climate information, on a selected domain that covers an area of interest. An RCM is nested within a GCM or global analyses of observations which provides the required large-scale conditions (the initial conditions (ICs) and the time dependant lateral boundary conditions (LBCs)) (Fennessy and Shukla, 2000). The RCMs produce high resolution simulation of surface variables which are affected by vegetation, land use and topographic features that can vary substantially over spatial scales of a few kilometers (Kim et al, 2000). Regional climate simulations are more than an interpolation of the lower resolution data from GCMs or the reanalyses. Regional climate modelling exploits the four-dimensional dynamics of the model, which account for the interaction of mesoscale circulations with a high-resolution representation of the local topography (Druyan et al, 2002). The RCMs, therefore, also offer a chance of understanding the regional climate better because they use physically and dynamically consistent ways (Kim et al, 2000).

The RegCM3 is the third generation RCM developed at the Abdus Salam International Centre for Theoretical Physics (ICTP) in Italy. The first generation National Centre for Atmospheric Research (NCAR) RegCM was built upon the NCAR-Pennsylvania State University Mesoscale version MM4 in the late 1980s. The dynamical component of the model originated from that of the MM4, which is a compressible, finite difference model with hydrostatic balance and vertical σ-coordinates. For application of the MM4 to climate studies, a number of physics parameterizations were replaced, mostly in the areas of radiative transfer and land surface physics, which led to the first generation RegCM. A first major upgrade of the model physics and numerical schemes was documented by Giorgi et al (1993a; 1993b), and resulted in the second generation RegCM (RegCM2). The physics of the RegCM2 was based on that of the NCAR

Community Climate Model 2 (CCM2), and the mesoscale model MM5 (Grell et al, 1994).

There have been several improvements and additions to the newest version of the RegCM3. In the last few years, some new physics schemes have become available for use in the RegCM, mostly based on physics schemes of the latest version of the Community Climate Model, CCM3 (Kiehl et al, 1996). First the CCM2 radiative transfer package was replaced by that of the CCM3. Changes in the model physics include a new large-scale cloud and precipitation scheme which accounts for the sub grid-scale variability of clouds (Pal et al, 2000) and new parameterizations for ocean surface fluxes (Zeng et al, 1998). The model has 18 sigma levels in the vertical and the cumulus parameterization scheme used in this experiment is Grell with the Fritsh and Chappell closure (Grell, 1993).

Initial Conditions (ICs) and Lateral Boundary Condition (LBC) fields are derived by standard interpolation procedures from the ECHAM4.5 data grid to the RegCM3 grid. The USGS Global Land Cover Characterization and Global 30 Arc-Second Elevation datasets are used to create the terrain files. The monthly optimum interpolation sea-surface temperature (OISST) analysis will be used as surface boundary conditions and these are produced weekly on a 1-degree grid. For the purposes of this experiment the RegCM3 model is run with a horizontal resolution of 60 km.

The period of interest in the study is DJF. The model is allowed to run for a period of about one month prior to the period of interest for spin-up purposes (Anthes et al, 1989). The atmosphere spins up rather quickly (within a few days), meaning the regional model dynamics equilibrate with the boundary forcing. The land, and in particular the soil moisture, can take much longer to spin up. Depending on how the soil moisture is initialized, it can take weeks to months to equilibrate (Giorgi and Mearns, 1999). The RCM climatology is determined by a dynamical equilibrium among the LBC forcing, the model-generated forcing from the interior of the domain, and the internal model physics and dynamics (Giorgi and Bi, 2000). Studies by Qian et al (2004) and Pan et al (2000) have shown that reinitialization improves the simulations because the simulations do not drift downstream. In this study we use a spin up period of one month to allow the land to spin-up and also to allow a long enough lead time that can be used in operational forecasting. November is used for model spin-up and the ensemble members of the NCEP driving fields are determined using a lagged (24-hour) average forecasting technique (Hoffman and Kalney, 1983). For nesting into the GCM fields, November 1 is the first simulation date, and for the reanalyses fields, the nested runs are started on 1, 2, 3 and 4 November.

The selection of the domain requires careful consideration. Seth and Giorgi (1997) suggested that in sensitivity studies the domains should be put well outside the area of interest so as to give the RCM solution the opportunity to respond to the internal physics and dynamics of the RCM. In some studies it was suggested that the important sources that influence the climate systems of the area of interest should be included in the domain (Fennessy and Shukla, 2000; Giorgi and Mearns, 1999). Southern Africa is influenced, amongst others, by the distant ENSO phenomenon. For skilful simulations, ENSO related information should be provided to the RCM at the lateral boundaries (Fennessy and Shukla, 2000). Most of the moisture that provides the rainfall in South Africa is advected from the Atlantic Ocean, the Indian Ocean and the Tropics (Cook et al, 2004; D’Aberton and Lindesay, 1992). During synoptic wet spells, moisture flux from the tropical and sub-tropical south-western Indian Ocean increases, and the heat low pressure system over Angola/Namibia may act as a tropical source for major synoptic rain producing systems such as tropical temperate troughs. The domain of interest for South Africa should include Madagascar because it affects the moisture flux from the Indian Ocean into South Africa and it also influences the migration of the cyclone-like vortices (Landman et al, 2005). With the consideration of the abovementioned facts the model domain is chosen to cover the area from about the equator to 40° S and from Greenwich to 40°E (Figure 2.5).

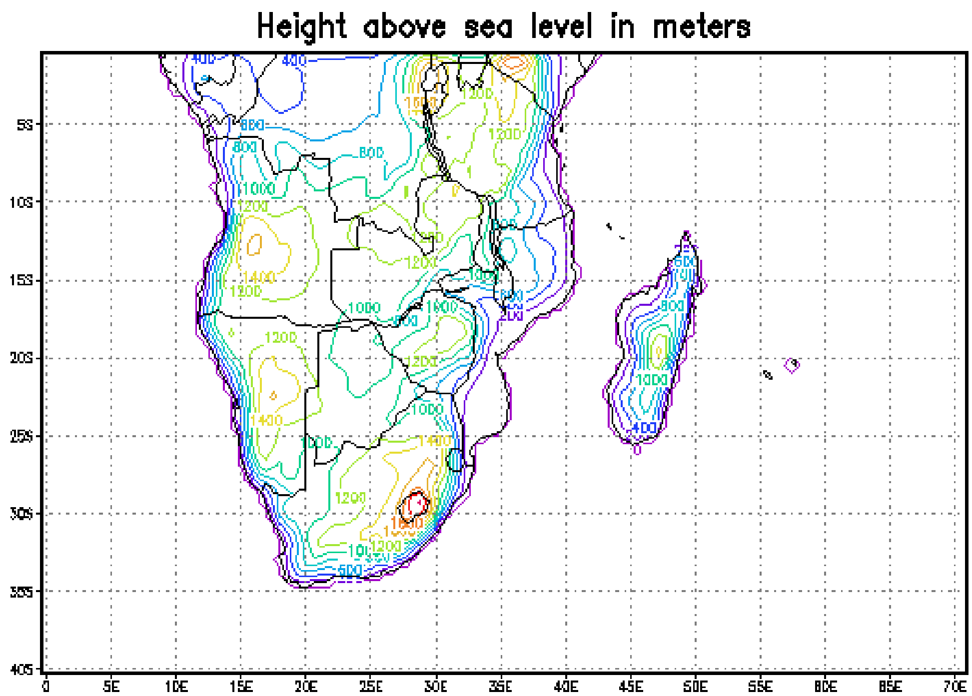

Figure 2.5. RegCM3 topography (meters above sea level) and domain of southern Africa.

Owing to computing and data storage constraints, RCM runs with only four ensemble members nested in ECHAM4.5 GCM large-scale fields (6-hourly data), and four ensemble members nested in NCEP reanalysis data (6-hourly data), are completed for the DJF seasons over a ten-year period from 1991/92 to 2000/2001. The large-scale forcing fields are from both the GCM and reanalysis data so that the performance of the two nesting systems can be compared and conclusions drawn on how the RCM is constrained by the large-scale conditions provided by the GCM.

2.4. Interpolation to stations and regions

An interpolation scheme is used to interpolate GCM and RCM output to the 963 stations and to 8 homogeneous regions. The technique is a superior alternative to those interpolation functions that assign the station value only from the nearest grid point. The algorithm, based on the inverse distance weighted interpolation method, detects four grid points nearest to a given station, and assumes that the interpolating surface is influenced by the nearby points (Shepard, 1968). The contribution from each grid point is evaluated using a weighting function which assigns the respective merit of each participant grid point according to its relative proximity to the station. The method also considers the extreme case where a station falls perfectly on the model grid point. Under this condition, it directly assigns the value to the station.

2.5. Canonical correlation analysis

The statistically based method used in constructing the base-line forecast model that uses SSTs as predictors (Landman and Mason, 1999) and the MOS models (Landman and Goddard, 2002) is called canonical correlation analysis (CCA). Canonical correlation analysis, which is often used as a forecast technique, is a multivariate statistical methodology to determine linear combinations of two data sets (the predictor data set, e.g. sea-surface temperature, and the predictand data set, e.g. observed rainfall) that are highly correlated, and is at the top of the regression modeling hierarchy (Barnett and Preisendorfer, 1987).

Canonical correlation analysis is used to seek relationships between two sets of variables. It attempts to find the optimum linear combination between the two sets with maximum correlation being produced. Because the predictor and the predictand fields contain a large number of highly correlated variables and few observations, it is recommended that pre-orthogonalization (Barnston, 1994) using standard empirical orthogonal function (EOF) analysis (Jackson, 1991) be performed. The predictor and predictand data sets are first standardized, resulting in correlation matrices on which the EOF analysis is performed. The standardization ensures that all the grid points and rainfall indices have equal opportunity to participate in the prediction process (Jackson, 1991; Barnston, 1994). EOF-analysis is performed separately for each of the predictor and predictand fields.

The number of modes to be retained in the analysis (i.e. those that will be used in the CCA eigenanalysis problem) is determined using forecast skill sensitivity tests. This is performed by cross-validation with varying numbers of retained predictor and predictand EOF modes. The combination producing the highest area-average correlation is used as the best estimate of the number of predictor and predictand EOF modes. For the predictor and predictand, the retained EOF modes usually explain about 60 - 80% of the variances. The truncation for the number of CCA modes retained is determined by using the Guttman-Kaiser criterion (Jackson, 1991) where only those modes having an eigenvalue greater that the average eigenvalue are retained. In most cases, this results in two CCA modes.

2.6. Model output statistics

Model output statistics (MOS) (Wilks, 1995) applied to GCM output can improve seasonal rainfall forecasts over southern Africa (Landman and Goddard, 2002). However, the question of whether or not the selection of a particular domain configuration has a significant impact on the simulation of seasonal climate rainfall anomalies over the region has remained largely unanswered. Since domain selection using dynamical downscaling techniques has a definite influence on forecast skill, investigation into the domain configuration using statistical downscaling methods is warranted. ECHAM4.5 GCM simulation (simultaneous observed SSTs serve as the lower boundary forcing) rainfall data (24 ensemble member mean) for the DJF season are used in the analysis. MOS is subsequently applied to the raw GCM rainfall data for a number of domain configurations (Figure 2.6).

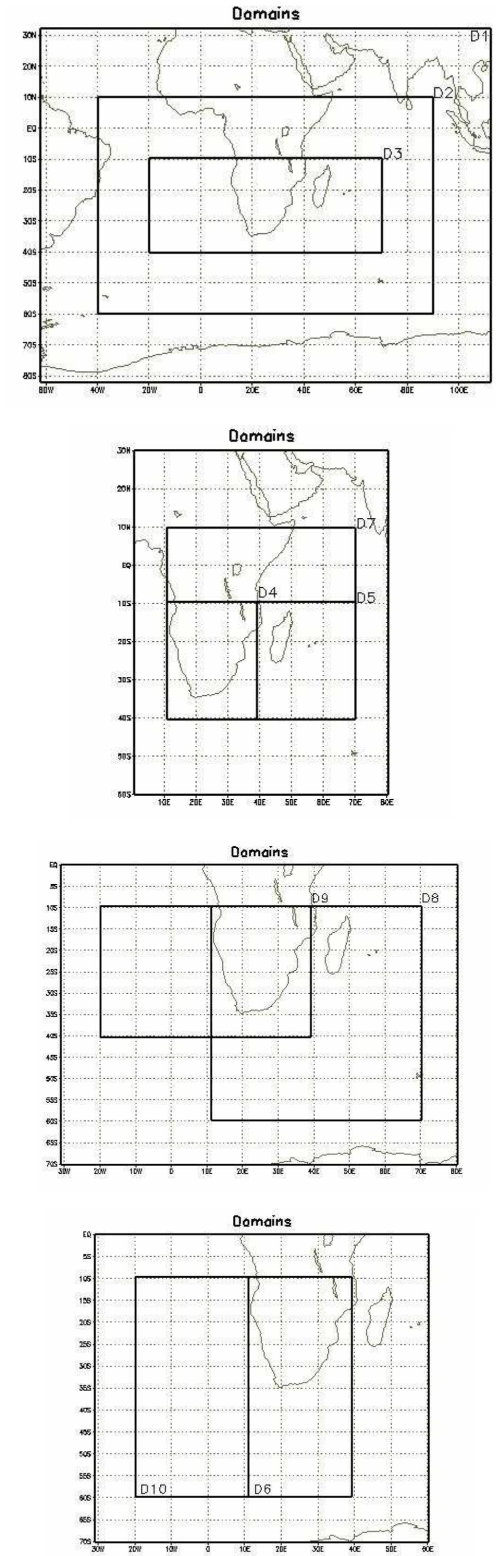

Figure 2.6. The 10 domain configurations considered in the MOS analysis.

The performance of the MOS system was judged deterministically using the area-averaged correlation between MOS-simulated rainfall for each homogeneous region of Figure 2.1 and the relevant observed rainfall index. Simulations were obtained using a 9-year-out cross-validation procedure that resulted in a 33-year test period from 1965/66 to 1997/98. First, an optimal linear statistical MOS model (i.e., the MOS model producing the highest averaged correlation over the summer rainfall regions) was designed for each domain.,Second, the best MOS model from each domain was subsequently compared and the domain with its MOS model producing the highest average correlation was considered to be the optimal domain of those considered here. A domain representing the equatorial Pacific Ocean was also considered on its own and in combination with the optimal southern African domain. The optimal African domain produced a MOS model that outperformed the MOS model that included the equatorial Pacific Ocean domain. The ability of the GCM to adequately simulate ENSO teleconnection patterns over southern Africa has therefore been demonstrated.

Table 2.1 shows the area averaged cross-validation correlations for the summer (DJF) rainfall regions. Domain 8 produced the best results. This domain is large enough to include the part of the south-western Indian Ocean that has an effect on southern African austral summer rainfall (Reason 2001).

D1	D2	D3	D4	D5	D6	D7	D8	D9	D10
0.381	0.351	0.365	0.365	0.384	0.406	0.388	0.407	0.345	0.348

Table 2.1. Area-averaged cross-validation correlations for the various domain configurations considered.

In this study the performance of both the SST baseline model and the ECHAM4.5-MOS model were tested over a multi-decadal time period using a 3-year-out cross-validation approach. The 10-year test period of 1991/1992 to 2000/2001 was subsequently extracted from the long cross-validated period.

2.7. Synopsis

The various simulation models and downscaling procedures have been described. They include the GCM, RCM, statistical base-line model, and MOS technique. The observed South African station rainfall data and how these data can be assigned to a number of homogeneous rainfall regions have also been described.

CHAPTER 3:
SIMULATION SKILL FOR REGIONS

3.1. Introduction

The aim of designing homogeneous rainfall regions is to group the rainfall stations into regions with similar interannual rainfall variability. Within each region, the mechanisms responsible for the rainfall variability should then be similar (Mason, 1998). Such a grouping should reduce some of the noise associated with individual stations and may as a result improve on simulation and forecast skill over the area of interest (Gong et al., 2003). In this chapter, the simulation skill over the 10-year period from 1991/92 to 2000/01 for each of the different simulation methods is compared. The simulation skill may be considered as an upper boundary for the various systems' operational forecasting potential.

3.2. Homogenous regions of the GCM and RCM

GCM and RCM output data were averaged over the grid-points located within each of the regions specified in Figure 2.1. The resulting time series were subsequently normalised over the 10-year test period. Figures 3.1 and 3.2 show where the grid-points of the GCM and RCM are allocated for each region. The representation of the homogeneous rainfall regions is better for the finer resolution nesting system than for the GCM. This difference in the horizontal resolution of the model may have an effect on calculating the rainfall time series representing the defined regions. Notwithstanding, this issue of model resolution is not considered in the report.

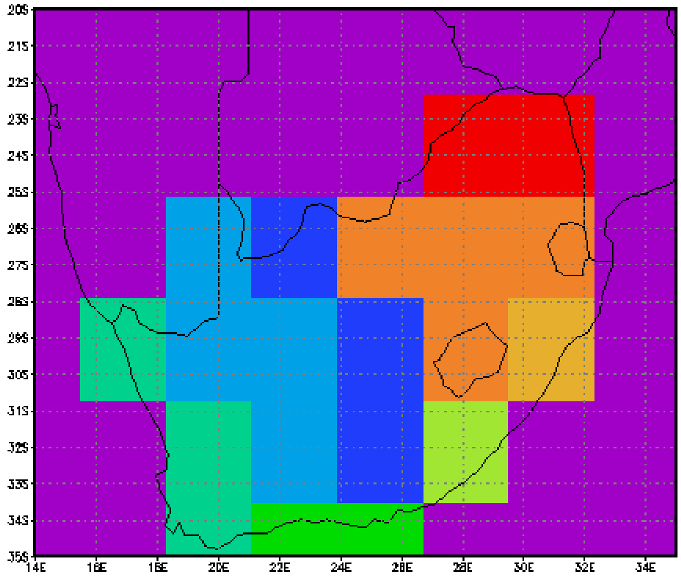

Figure 3.1. Grid-point allocation of the ECHAM4.5 to the homogeneous rainfall regions.

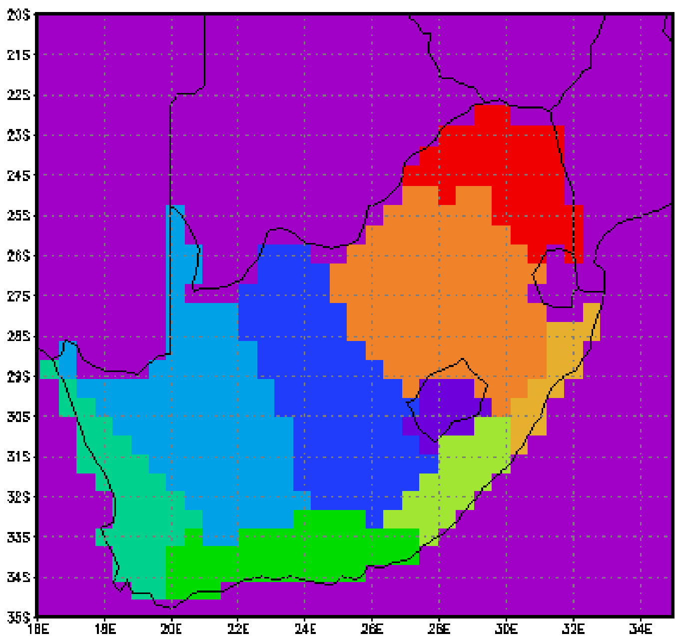

Figure 3.2. Grid-point allocation of the RegCM3 to the homogeneous rainfall regions.

3.3. Simulation skill levels for the 10-year period

With such a small ensemble (4 members for the GCM-RCM nesting), it was unrealistic to expect to be able to derive useful conclusions based on the ensemble distribution. For this reason ensemble mean values were used and simulation skill levels compared by considering only Pearson (“ordinary”) correlation values that reflect the strength of linear relationships. Unfortunately, owing to these constraints and the short test period of 10 years, it was not possible to demonstrate unequivocally that one simulation method is better than the other. Notwithstanding, the results obtained should be able to demonstrate the relative potential of the methods used to simulate seasonal rainfall during the 1990s.

The various simulation methods used were:

1. DJF SST to simulate DJF rainfall;
2. Raw ECHAM4.5 DJF rainfall simulation data using the mean of the full ensemble of 24 members;
3. Raw ECHAM4.5 DJF rainfall simulation data using a 4-member ensemble mean derived from a large number (500) of Monte Carlo iterations;
4. ECHAM4.5-MOS DJF rainfall simulation data using the mean of the full ensemble of 24 members;
5. ECHAM4.5-MOS DJF rainfall simulation data using a 4-member ensemble mean derived from a large number (500) of Monte Carlo iterations; and,
6. ECHAM4.5-RegCM3 nested DJF rainfall simulation data using a 4-member ensemble mean.

Since the skill comparison may be biased when simulation methods using different ensemble sizes are compared, a Monte Carlo procedure (Wilks, 1995) was applied to the raw ECHAM4.5 and ECHAM4.5-MOS ensemble in order to randomly select 4 ensemble members a large number of times (500) and then calculate the average ensemble mean over the large number of iterations. In this way, the possibility of selecting the best (or worse) set of 4 members to be used in the skill comparisons was eliminated. The full iteration set was subsequently used to calculate 95% confidence intervals using the normal distribution.

3.3.1. Regional skill levels

Correlation values for each of the 8 homogeneous regions obtained from the 6 simulation methods are shown in Figure 3.3. With such a small sample it proved very difficult to obtain results that are significant at the 95% level. Notwithstanding, the full raw ECHAM4.5 ensemble (24 members) for the northern KwaZulu-Natal region superceded this limit, and three more simulations (raw and ECHAM4.5-MOS for the Lowveld, and raw ECHAM4.5 using the full ensemble for the central interior) achieved 90% confidence status. Moreover, the baseline skill level of the SST-forced statistical model was outscored, even over the far north-eastern areas (northern KwaZulu-Natal and the Lowveld) where the baseline model was found to produce the highest skill.

For a majority of the regions, with the exception of the southern coast, Lowveld and western interior, the raw ECHAM4.5 skill was higher than the ECHAM-MOS skill. This result is in contrast to what has been found when applying a MOS procedure to an older (Landman and Goddard, 2002) and a later (Shongwe et al. 2006) version of the ECHAM GCM where MOS skill has been demonstrated to be higher than raw model output skill. The apparent discrepancy may be a result of the much shorter period of 10 years used here as opposed to the testing periods of several decades used in the earlier papers. This result reemphasizes the statement made earlier that it will be hard to demonstrate unequivocally that one simulation method is better than the other when using such a small sample.

Notwithstanding the sample size, for each of the regions the performance of the simulation system with the larger ensemble was better than when using a subset of the full ensemble (raw ECHAM4.5 (24) vs. raw ECHAM4.5 (4); ECHAM4.5-

MOS (24) vs. ECHAM4.5-MOS (4)). This result is to be expected since ECHAM4.5 skill improves over southern Africa until 16 members have been considered (section 2.2), and improvement in skill with larger ensemble sizes has been demonstrated elsewhere (e.g., Krishnamuti et al. 2000).

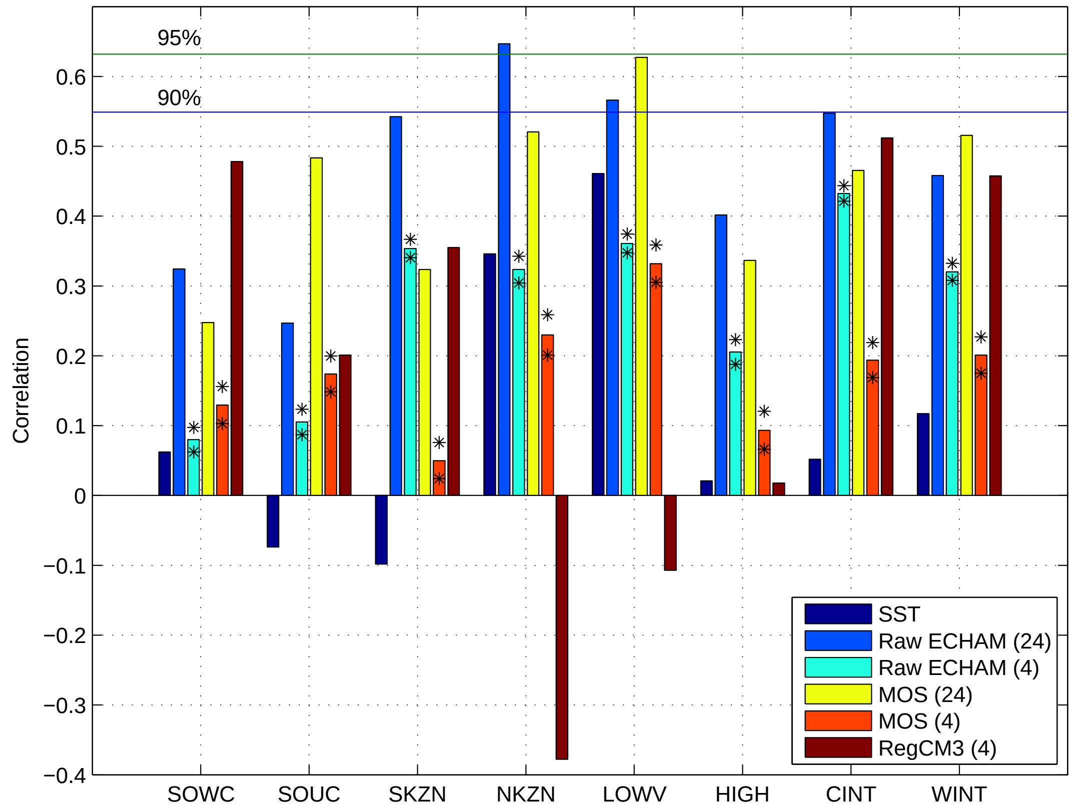

Figure 3.3. Simulation skill (correlation) for each region using the 6 simulation methods. Horizontal lines indicate the 90% and 95% confidence levels. Asterisks show the 95% confidence intervals obtained from the Monte Carlo process.

Performance of the ECHAM4.5-RegCM3 system was relatively high over the central and western parts of the country. In fact, the best skill for the south-western Cape was from the nested system. With the exception of northern KwaZulu-Natal, the Lowveld and the Highveld where negative or near-zero correlations were found, the nested system produced skill levels that are higher than those obtained from the ECHAM4.5 and ECHAM4.5-MOS simulations using the small ensemble (4 members). The negative correlations found for KwaZulu-Natal and the Lowveld may be attributed to steep topographic gradients in the area since the RegCM3 tends to overestimate rainfall over such gradients (see Chapter 5). However, owing to the improvement in skill with larger ensemble sizes, the demonstrated simulation performance of the ECHAM4.5-RegCM3 should improve for all the regions with an increasing ensemble size.

The spatial distribution in simulation skill is demonstrated in Figure 3.3 above. Figure 3.4 shows the performance of the simulation methods over the 10-year test period averaged over the 8 regions. The time series of the figure are standardized departures. Correlation values associated with the raw ECHAM4.5 and MOS methods are high and between 0.6 (above 90% confidence) and 0.7 (above 95% confidence), with the correlation associated with the nested system 0.5, followed by the SST baseline model of 0.2. Simulated anomalies are generally overestimated during the El Niño season of 1997/97 and the La Niña season of 1998/99, while the wet conditions during 1995/96 are underestimated. The rainfall during the 1999/2000 La Niña season is skillfully simulated by most of the systems, especially by the ECHAM4.5-MOS system.

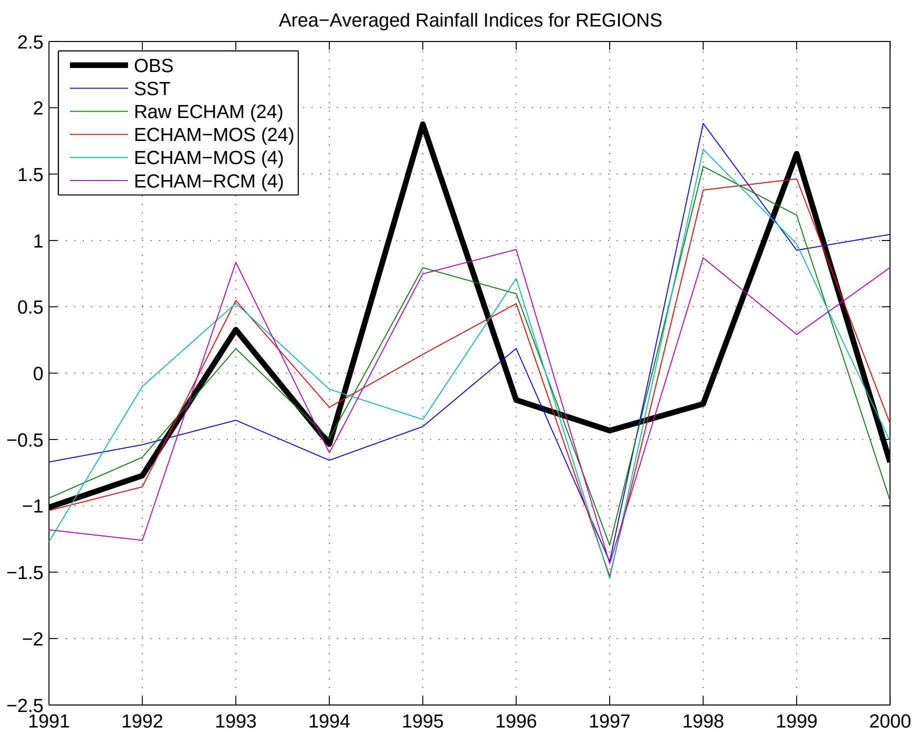

Figure 3.4. Regional area-averaged simulation performances over the 10-year test period.

3.3.2. Post-processing nested simulations

The advantages of statistically correcting dynamical model output has been demonstrated in the literature (e.g., Landman and Goddard, 2002) and also partly demonstrated above. Figure 3.5 shows the result of doing a 1-year-out cross-validation procedure over the 10 years relating the simulated 850 hPa geopotential height field of the ECHAM4.5-RegCM3 system to the regional rainfall. The MOS process improved the correlation value from 0.5 to 0.6. However, a period longer than 10 years is required to test the robustness of the prediction equations.

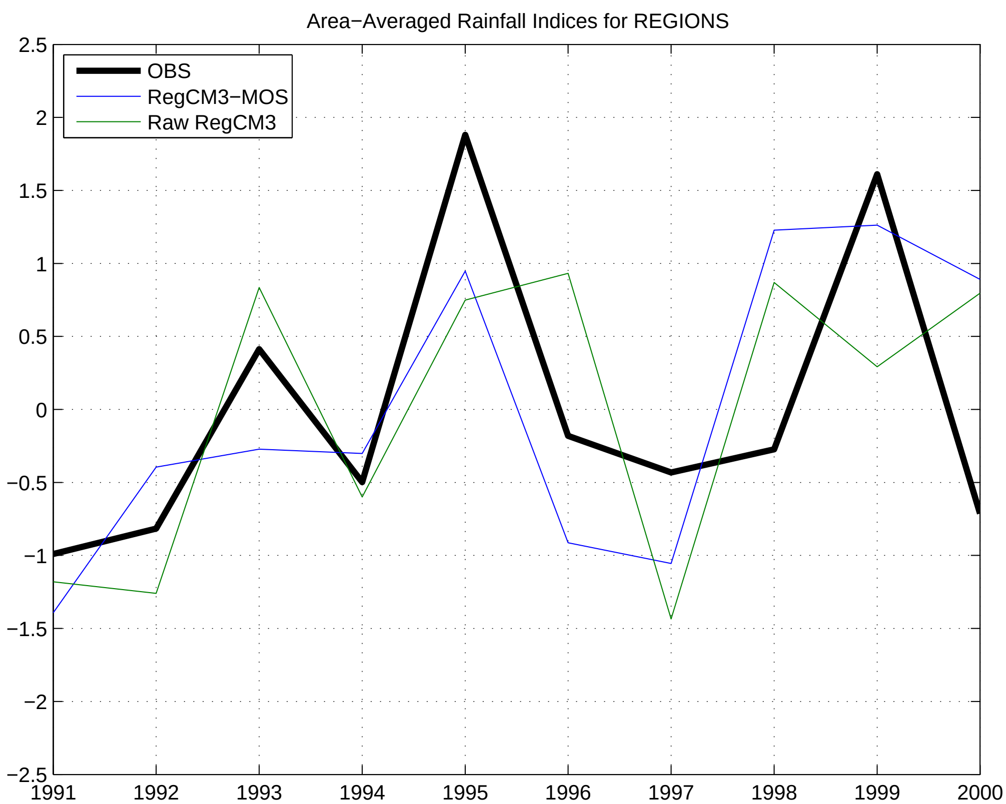

Figure 3.5. Regional area-average simulation performance of the raw ECHAM4.5-RegCM3 system and the ECHAM4.5-RegCM3-MOS system.

3.3.3. GCM vs. NCEP nesting

The skill of the nested system may be adversely affected by the large-scale driving fields (Chouinard et al., 1994). The RegCM3 was nested in the large-scale driving fields obtained from the NCEP reanalysis data set and its simulation skill compared with the skill from the GCM-RCM system. The results presented as regional area-averaged values are shown in Figure 3.6. The respective simulations compare well during the first half of the test period, but differences in nested-system performance are seen thereafter, with the exception of 1998/99. The NCEP nested system produced area-averaged simulations that show a high correlation with that observed (0.8), and does not show the anticipated negative rainfall anomaly usually associated with El Niño events over southern Africa and also simulated by the GCM-RCM system. This result suggests that improvement in GCM forecast skill may lead to improved nested simulations.

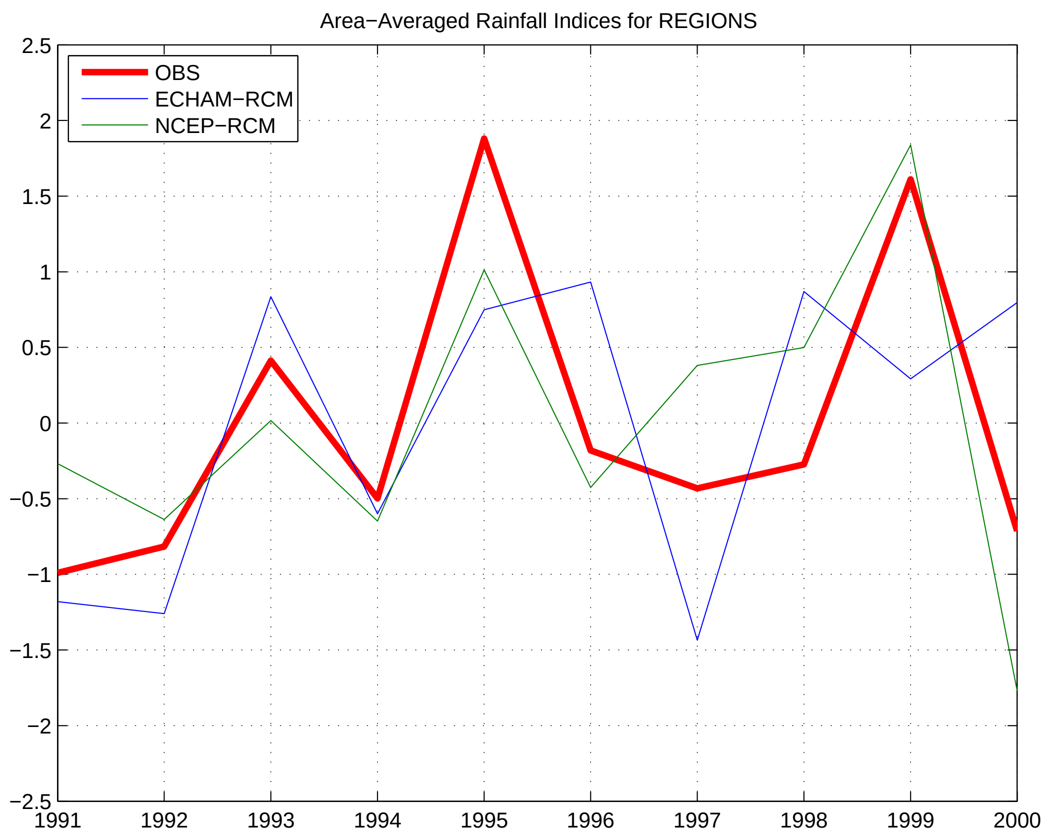

Figure 3.6. Regional area-average simulation performance of the ECHAM4.5-RegCM3 system and the NCEP-RegCM3 system.

3.4. Synopsis

Simulation skill for the 8 homogeneous rainfall regions has been demonstrated over the 10-year test period (1991/92 to 2000/01). Although this is a short period, consequently making it difficult to unequivocally state which simulation method is better than the other, useful conclusions can be drawn from the analyses. The following have been demonstrated:

1. The simulation systems involving GCM data outscore the baseline skill obtained from simulating rainfall using global SSTs;
2. Low nested-system skill is found over the north-eastern half of the country; however, skilful simulations are found for this part using raw GCM and GCM-MOS simulation methods;
3. The full GCM and GCM-MOS ensemble produces skill levels which are higher than the Monte Carlo 4-member subset, reemphasizing previous findings that increasing ensemble size improves model simulations;
4. Nested-system skill levels may be further enhanced with increasing ensemble size; and,
5. Nesting the RCM in reanalysis data produces better results than nesting the RCM in the GCM data, thereby providing an indication of how nested simulations are constrained by the boundary conditions provided by the GCM.

The potential for using dynamical and statistical downscaling methods for modelling South African seasonal regional rainfall variability has been demonstrated. Skill may be further improved with larger ensemble sizes for both types of downscaling approaches. The next chapter repeats most of the analyses performed here, but for stations as opposed to regions.

CHAPTER 4:
SIMULATION SKILL FOR STATIONS

4.1. Introduction

Although spatial aggregation of model output may improve on model performance, grouping large numbers of stations together obscures some of the characteristics of the simulations or forecasts unique to particular stations (Taylor and Leslie, 2005). As is the case in Chapter 3, the simulation skill over the 10-year period from 1991/92 to 2000/01 for each of the different simulation methods is again assessed, but for the 963 stations. In addition, the various simulation methods identified in section 3.3 are also used here to describe upper boundaries for the various systems' operational forecasting potential for single-stations.

The description of the various simulation systems' performance is described here in terms of their respective status in the hierarchy of the complexity of the systems. Complexity is defined according to the number of tiers involved in the simulation system as well as the computing requirements to perform the simulation. For example, a simulation system that uses only SST as predictor is less complex and hence has a lower status in the modelling hierarchy than a system involving post-processing of GCM large-scale fields. Moreover, when the same number of simulation tiers is involved, a regional modelling approach requires more computing resources than a statistical MOS approach and hence has a higher status. The systems are next discussed according to their status, and skill differences are calculated by subtracting skill of the lower status system from the skill of the higher status system.

Based on the above definition of model hierarchy, the simulation methods are ranked from the highest to the lowest status as follows:

1. GCM-RCM;
2. GCM-MOS;
3. Raw GCM; and,
4. SST as predictor.

4.2. Simulation skill levels for the 10-year period

4.2.1. Station skill levels

The station correlations between the simulations from the 6 systems and the observed rainfall are described here. The system with the highest status in the hierarchy is the GCM-RCM system, and its correlation map is shown in Figure 4.1. In general, the correlation values are low, with the majority of the station correlations less than 0.2. The low skill found here is in contrast to the results found for simulating the regional rainfall, where the south-western Cape and the central and western interiors are associated with correlation values higher than 0.4.

The GCM-MOS system (full ensemble) shows more encouraging results (Figure 4.2). The western and north-eastern parts have the highest correlation values, but low values are found over the Highveld region, which is in agreement with the regional skill assessment. The associations of the ECHAM4.5-MOS 4-member ensemble and the observed rainfall are shown in Figure 4.3. This figure also shows the upper and lower confidence limits of the 95% significance level, calculated using the normal distribution fitted to 500 Monte Carlo simulations selecting subsets of 4 members from the 24 member ensemble. In general, the same correlation distribution pattern is seen here, but with lower correlation values owing to the smaller ensemble size used.

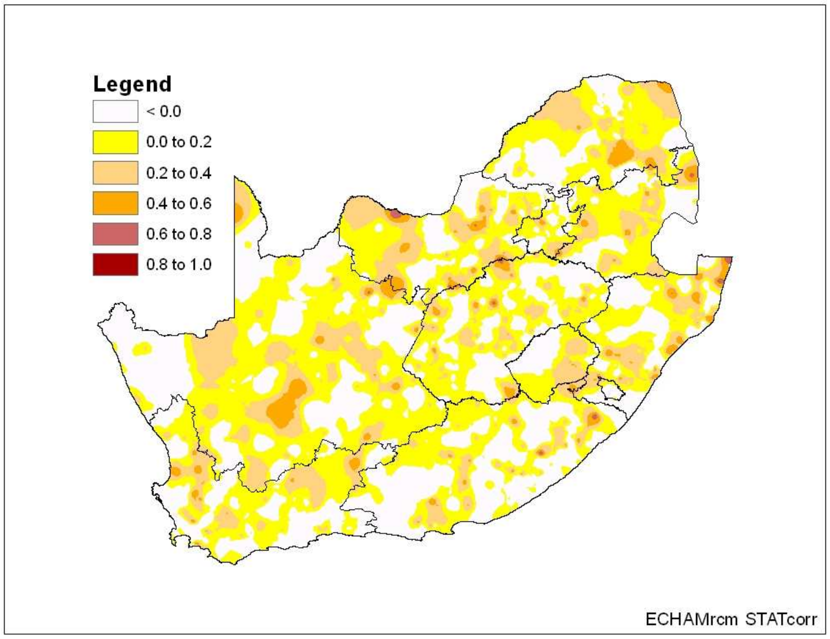

Figure 4.1. Correlations between the ECHAM4.5-RegCM3 rainfall simulation (4-member mean) and the observed rainfall over the 10-year test period of 1991/92 to 2000/01. Correlation values less than 0 are masked out.

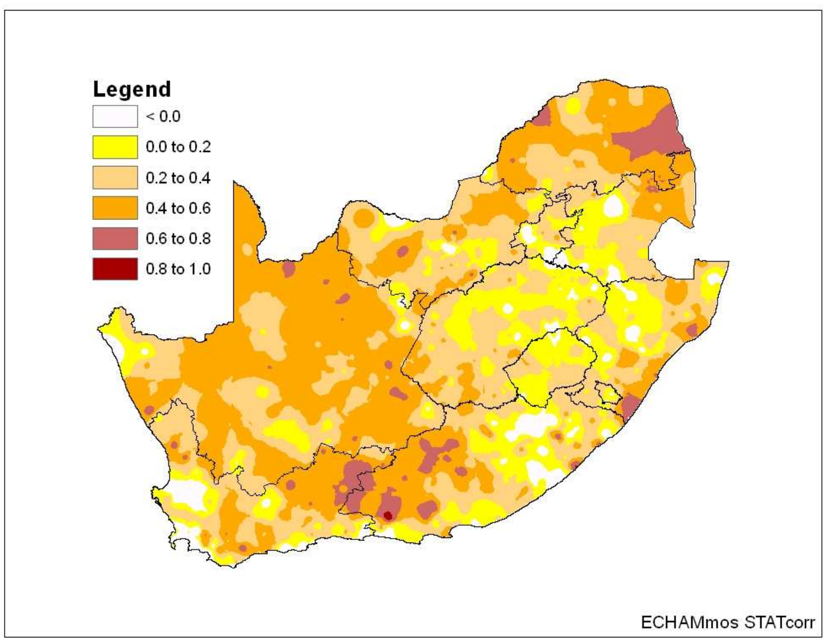

Figure 4.2. Correlations between the ECHAM4.5-MOS rainfall simulation (24-member mean) and the observed rainfall over the 10-year test period of 1991/92 to 2000/01. Correlation values less than 0 are masked out.

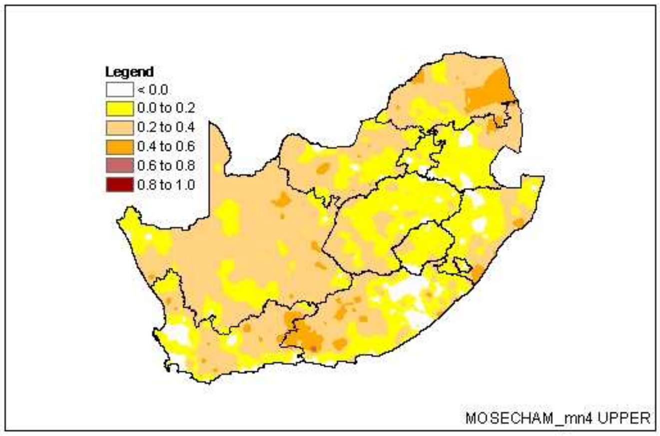

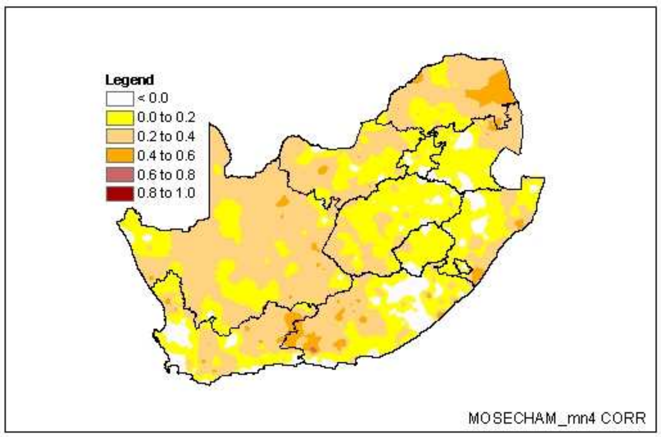

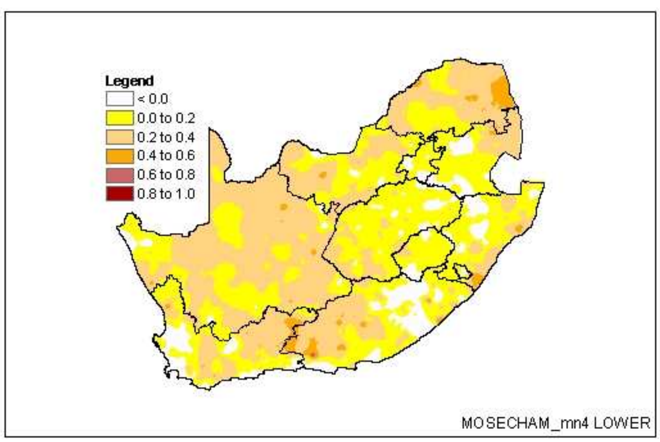

Figure 4.3. Correlations between the ECHAM4.5-MOS rainfall simulation (4-member mean) and the observed rainfall over the 10-year test period of 1991/92 to 2000/01. Correlation values less than 0 are masked out. The top panel shows the upper limit and the bottom panel the lower limit of the 95% significance level.

The raw ECHAM4.5 output (Figure 4.4) shows similar correlation patterns to the ECHAM4.5-MOS system of Figure 4.2. However, the raw GCM output produced higher skill over the western parts of the Eastern Cape Province to the south and over the Limpopo Province to the north. Low skill is found in between. It seems that the MOS makes its best contribution over the western parts of the country, but for some stations it causes the simulation skill of the raw GCM output to deteriorate.

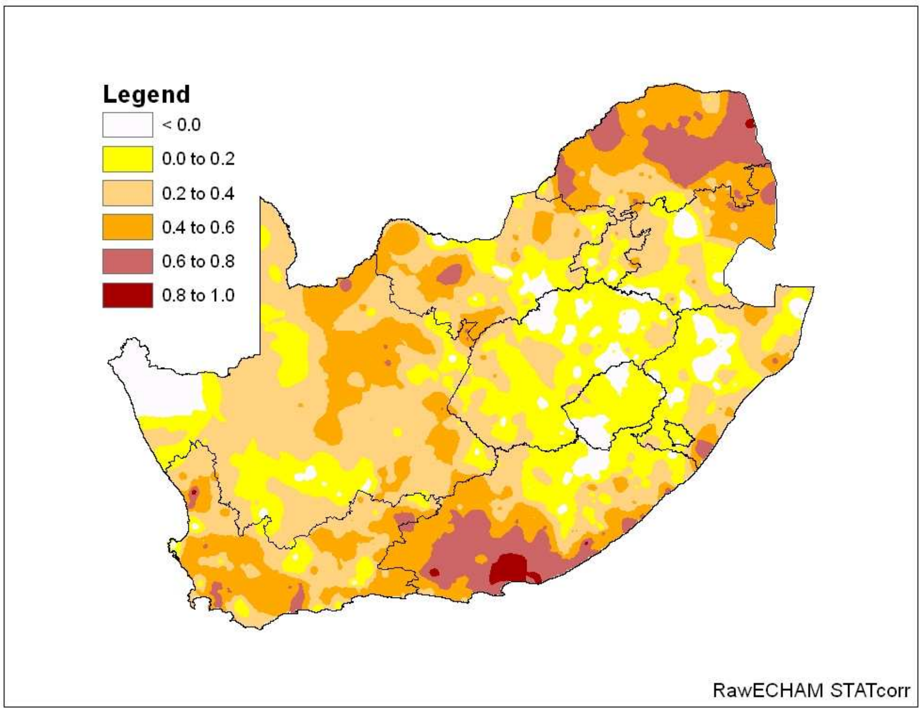

Figure 4.4. Correlations between the raw ECHAM4.5 rainfall simulation (24-member mean) and the observed rainfall over the 10-year test period of 1991/92 to 2000/01. Correlation values less than 0 are masked out.

The results of the raw ECHAM4.5 output using a 4-member ensemble are shown in Figure 4.5. Similar to the results obtained for the ECHAM4.5-MOS 24-member system, similar correlation patterns are found for the smaller ensemble, but with lower values owing to the smaller ensemble size.

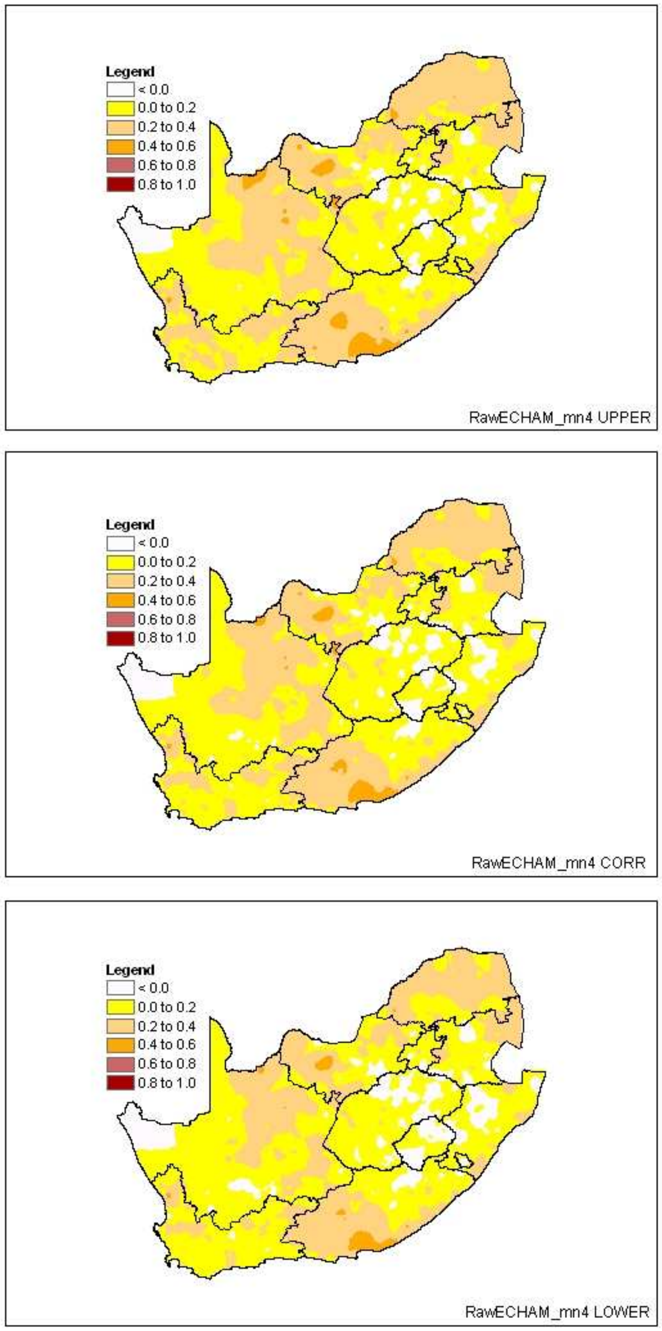

Figure 4.5. Correlations between the raw ECHAM4.5 rainfall simulation (4-member mean) and the observed rainfall over the 10-year test period of 1991/92 to 2000/01. Correlation values less than 0 are masked out. The top panel shows the upper limit and the bottom panel the lower limit of the 95% significance level.

Simulation skill obtained from the baseline system (Figure 4.6) is generally lower than the skill associated with the statistical post-processed simulations and the raw GCM output. The best skill is found over the far north-eastern parts and along the coastal regions of KwaZulu-Natal.

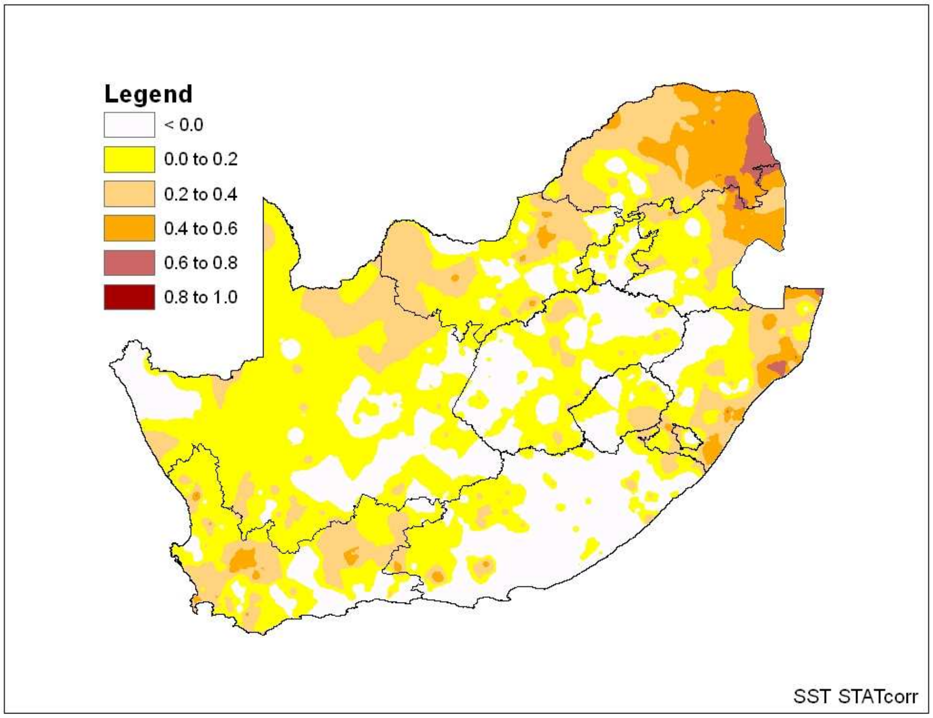

Figure 4.6. Correlations between the baseline model (using SSTs as predictor) and the observed rainfall over the 10-year test period of 1991/92 to 2000/01. Correlation values less than 0 are masked out.

The figures presented above show the associations between simulated rainfall and observed rainfall and present evidence that the highest skill is found over the north-eastern and central-western parts. Skill over the Highveld is the lowest. These results are in agreement with the results for the regional rainfall simulations. Although the simulation systems are in agreement with regard to where the best skill is found, the main purpose of this study is to compare the various downscaling systems. The next section shows maps of the correlation differences when comparing the simulation systems.

4.2.2. Skill differences over the 10-year period

This section presents correlation difference maps for the simulation systems. Lower ranked system (lower in the hierarchy described above) correlations are subtracted from higher ranked system correlations. For example, GCM-MOS simulation skill is subtracted from GCM-RCM values because the GCM-RCM has a higher rank. Negative correlation differences provide evidence that the more complex, higher ranked system, is performing poorer than the less sophisticated system. Six cases are presented here:

1. GCM-RCM minus GCM-MOS;
2. GCM-RCM minus Raw GCM;
3. GCM-RCM minus baseline model;
4. GCM-MOS minus Raw GCM;
5. GCM-MOS minus baseline model; and,
6. Raw GCM minus baseline model.

The most complex simulation system considered here involves the nesting of the RCM into the GCM large-scale fields. Figure 4.7 shows the correlation differences between the ECHAM4.5-RegCM3 system and the ECHAM4.5-MOS system using the full ensemble (24 members). Only isolated areas of positive correlation differences are found, with the largest concentration of positive differences restricted to the Highveld and central parts. This pattern is repeated in Figure 4.8, which shows the results from considering a 4-member ensemble. Comparing the ECHAM4.5-RegCM3 with the raw ECHAM4.5 skill levels (Figures 4.9 and 4.10) shows that the greater benefit of using the GCM-RCM system compared to the raw GCM data is mainly restricted to the Highveld and western areas; the least benefit is seen over the far southern parts. Notwithstanding the GCM-RCM's poor showing against these other systems, it outscores the baseline model over the larger part of South Africa (Figure 4.11), except over the far north-eastern parts where high skill is found using the baseline model (Figure 4.6).

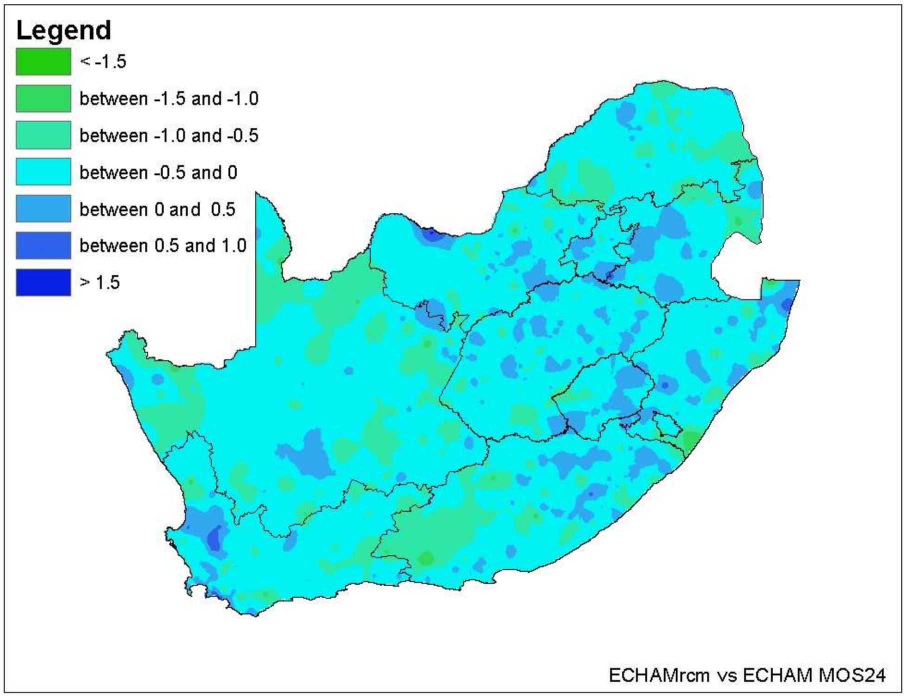

Figure 4.7. Correlation differences between the ECHAM4.5-RegCM3 system and the ECHAM4.5-MOS system (full set ensemble of 24) over the 10-year test period of 1991/92 to 2000/01.

The GCM-MOS system generally produces higher skill than the raw GCM simulations (Figures 4.12 and 4.13), with the exception the southern coastal and adjacent areas and to a lesser extent the far north-eastern parts. In addition, the ECHAM4.5-MOS system also outscores the baseline model over the larger part of South Africa, excluding the far north-eastern parts where SSTs produce high levels of skill (Figures 4.14 and 4.15). The baseline model is similarly outscored using raw ECHAM4.5 simulations (Figures 4.16 and 4.17).

Except for the GCM-RCM system, the higher ranked systems seem to outscore the lower ranked systems over the larger part of the country. This result is in contrast to the results of the regional skill assessments of Chapter 3 where useful skill from the nested system is demonstrated.

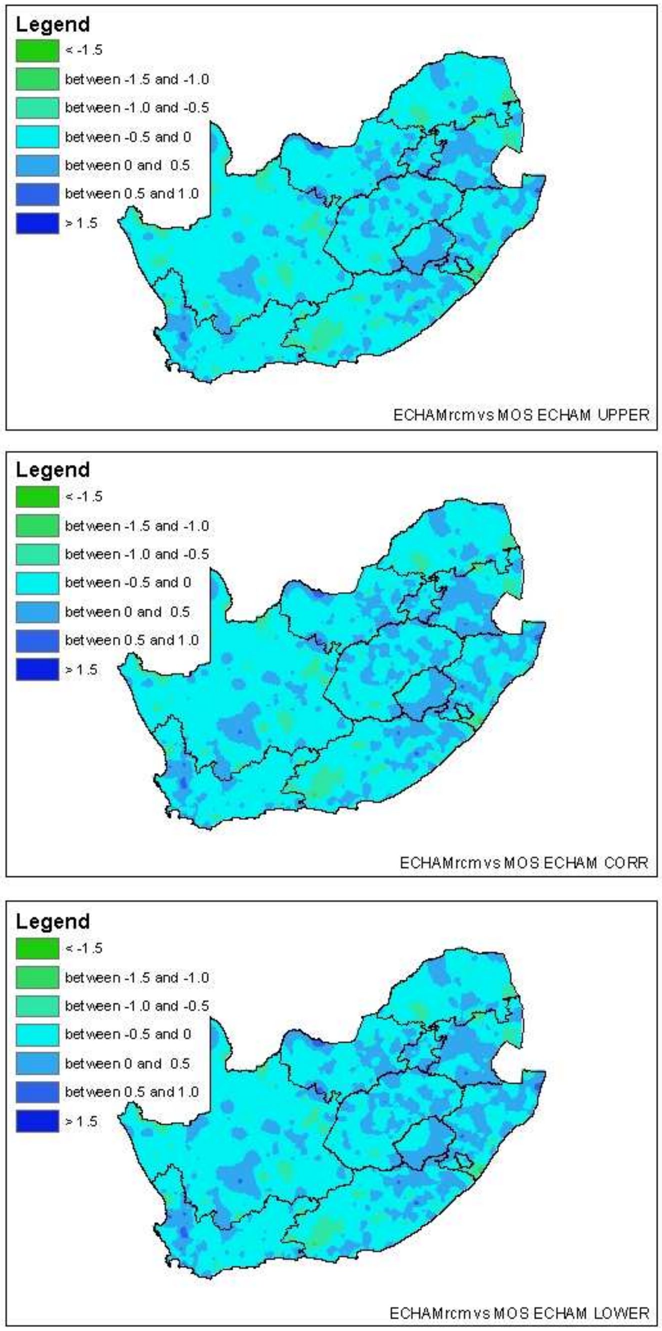

Figure 4.8. Correlation differences between the ECHAM4.5-RegCM3 system and the ECHAM4.5-MOS system (4 ensemble members) over the 10-year test period of 1991/92 to 2000/01. The top panel shows the upper limit and the bottom panel the lower limit of the 95% significance level.

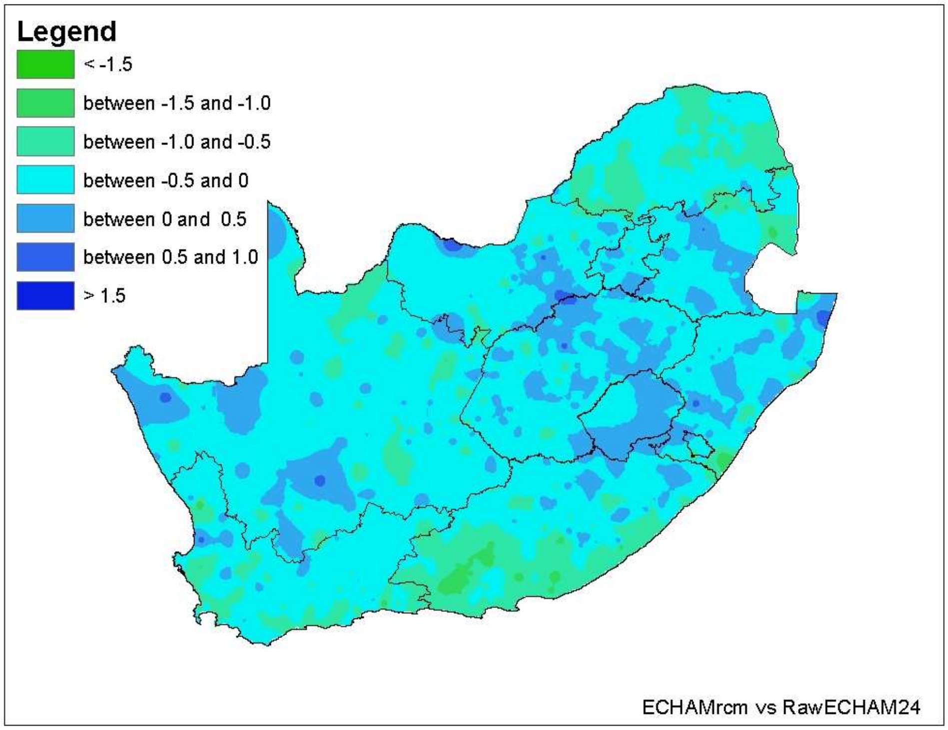

Figure 4.9. Correlation differences between the ECHAM4.5-RegCM3 system and the raw ECHAM4.5 system (full set ensemble of 24) over the 10-year test period of 1991/92 to 2000/01.

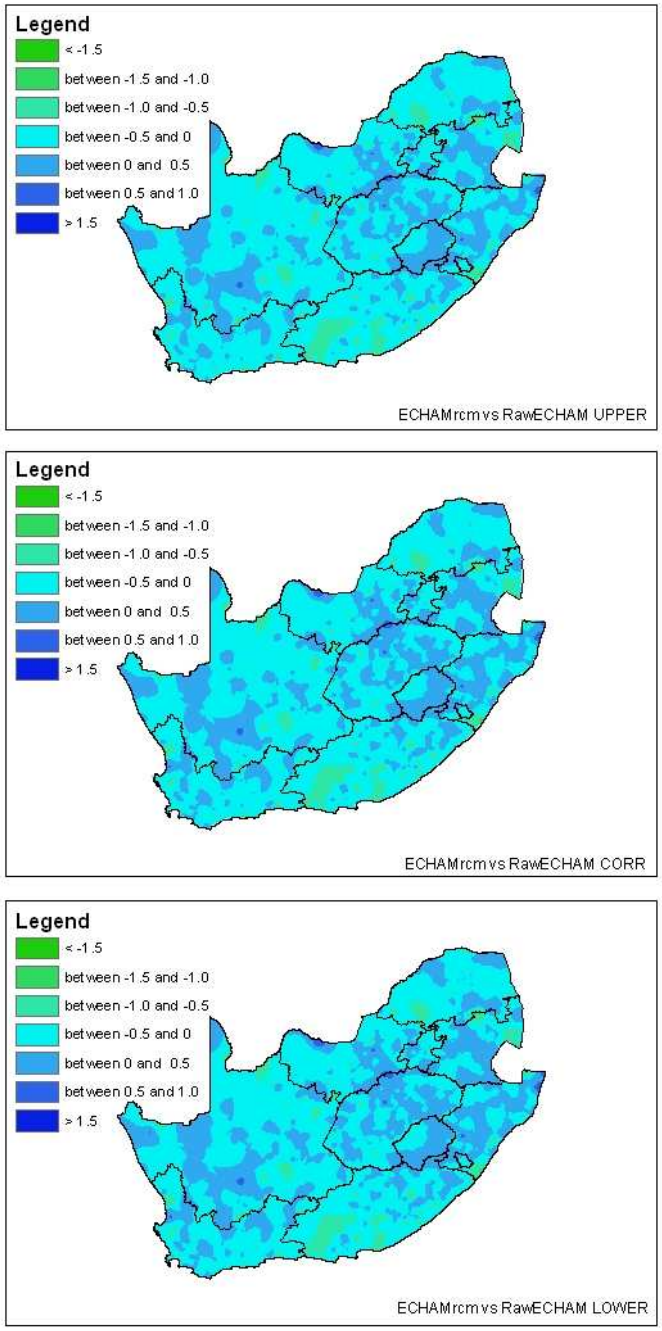

Figure 4.10. Correlation differences between the ECHAM4.5-RegCM3 system and the raw ECHAM4.5 system (4 ensemble members) over the 10-year test period of 1991/92 to 2000/01. The top panel shows the upper limit and the bottom panel the lower limit of the 95% significance level.

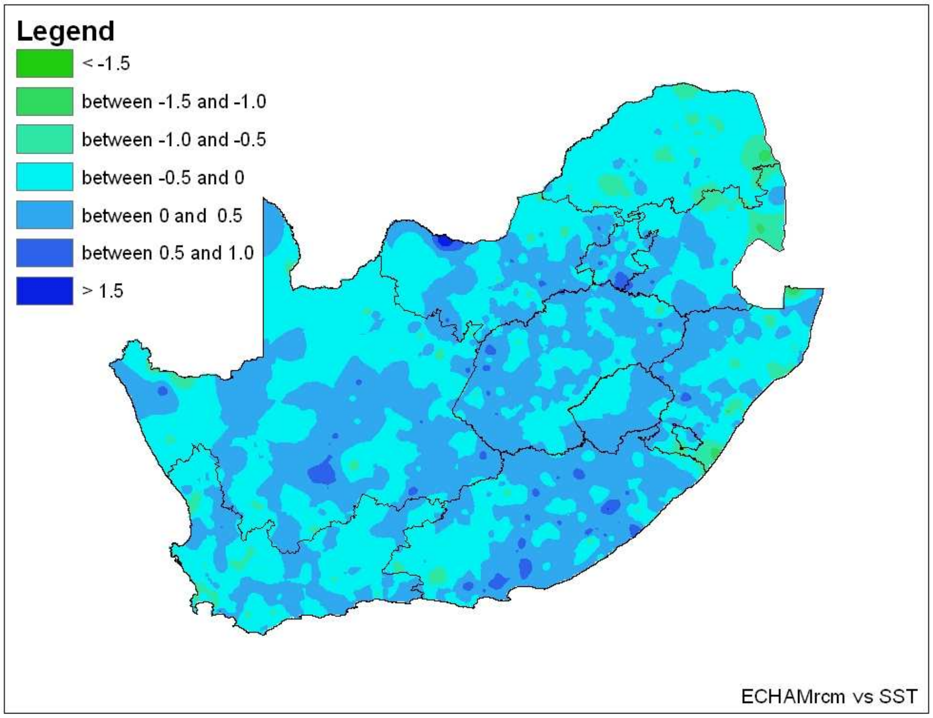

Figure 4.11. Correlation differences between the ECHAM4.5-RegCM3 system and the baseline model (using SST to simulate rainfall) over the 10-year test period of 1991/92 to 2000/01.

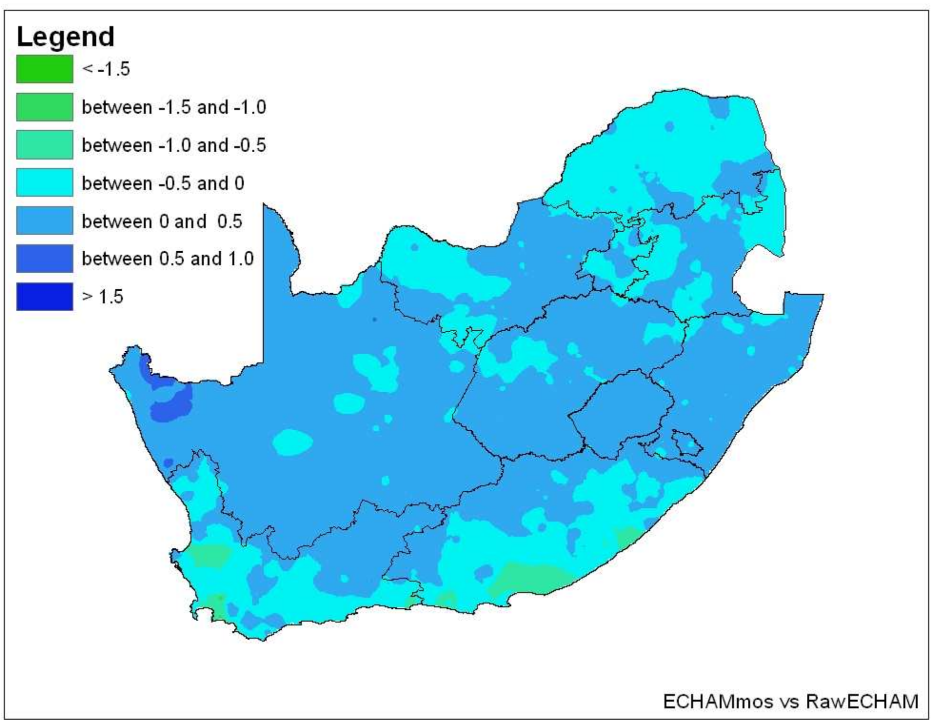

Figure 4.12. Correlation differences between the ECHAM4.5-MOS and raw ECHAM4.5 systems (full ensemble of 24) over the 10-year test period of 1991/92 to 2000/01.

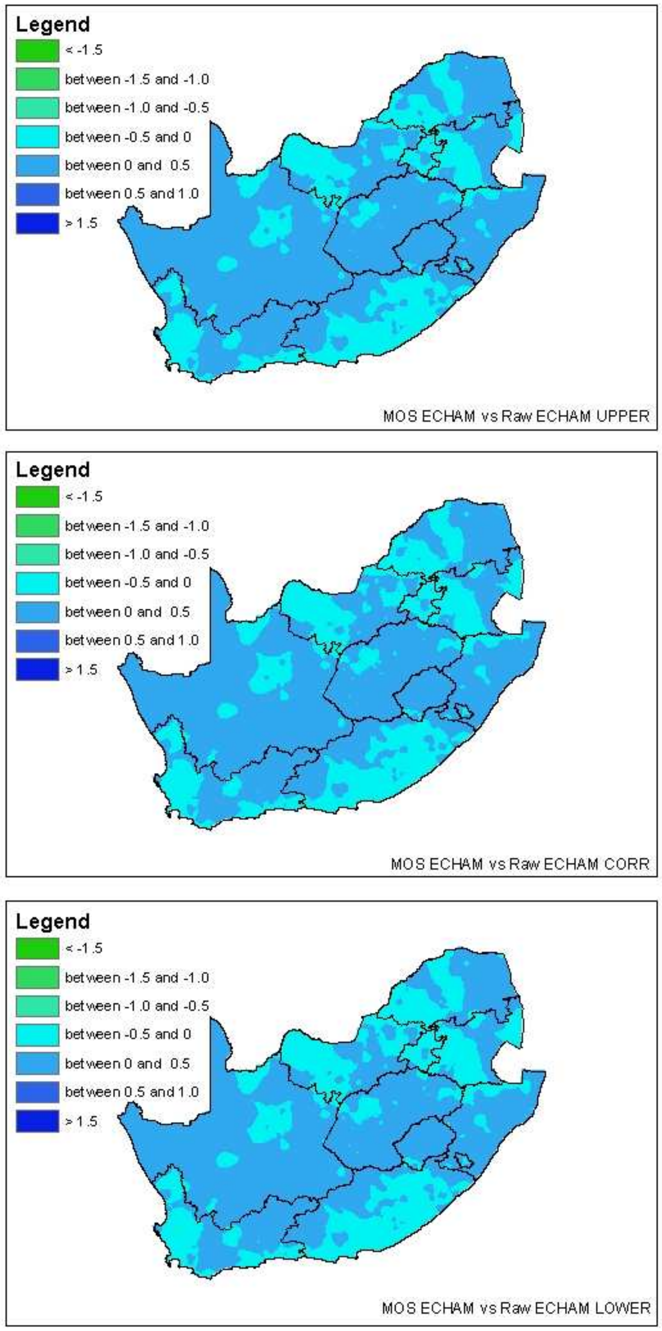

Figure 4.13. Correlation differences between the ECHAM4.5-MOS and raw ECHAM4.5 systems (4 ensemble members) over the 10-year test period of 1991/92 to 2000/01. The top panel shows the upper limit and the bottom panel the lower limit of the 95% significance level.

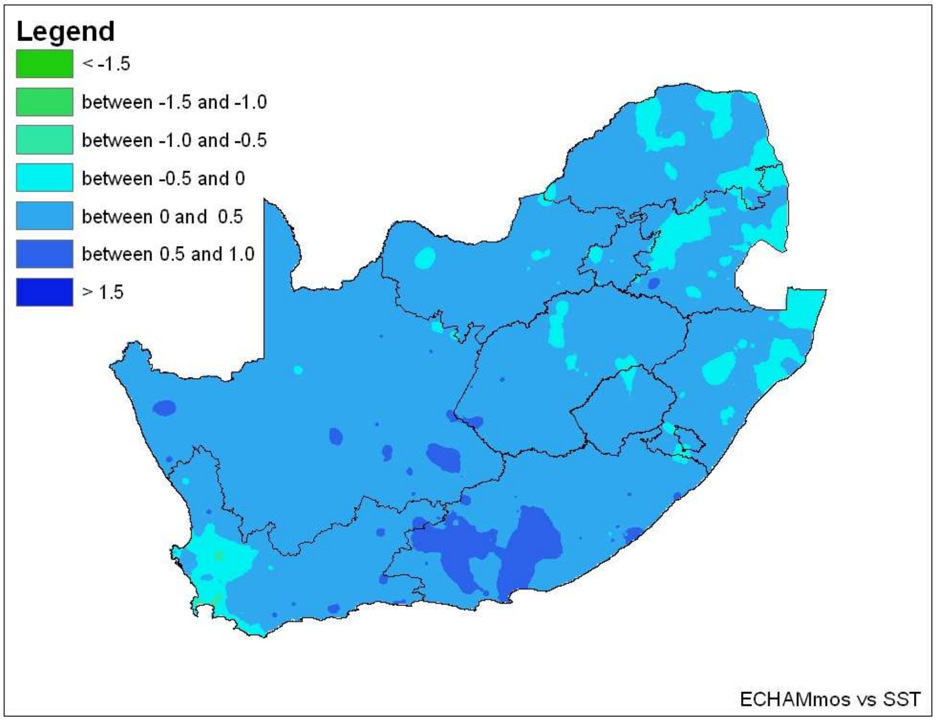

Figure 4.14. Correlation differences between the ECHAM4.5-MOS (full ensemble of 24) and the baseline system (SST as predictor) over the 10-year test period of 1991/92 to 2000/01.

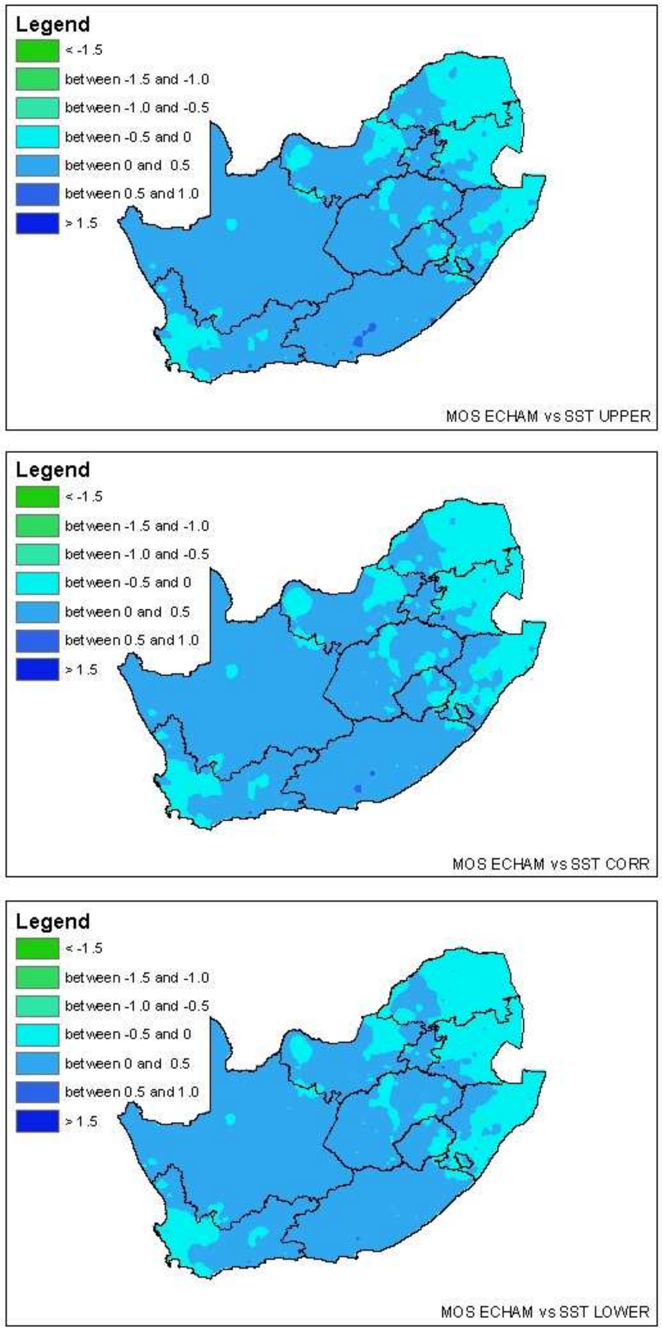

Figure 4.15. Correlation differences between the ECHAM4.5-MOS (4 ensemble members) and the baseline model (SST as predictors) over the 10-year test period of 1991/92 to 2000/01. The top panel shows the upper limit and the bottom panel the lower limit of the 95% significance level.

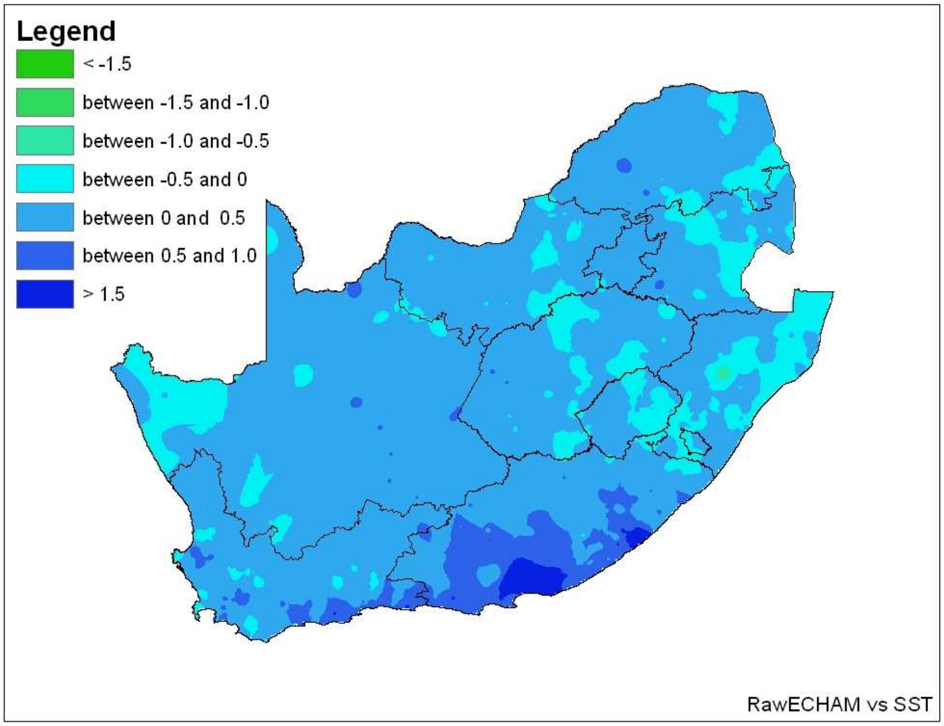

Figure 4.16. Correlation differences between the raw ECHAM4.5 (full ensemble of 24) and the baseline system (SST as predictor) over the 10-year test period of 1991/92 to 2000/01.

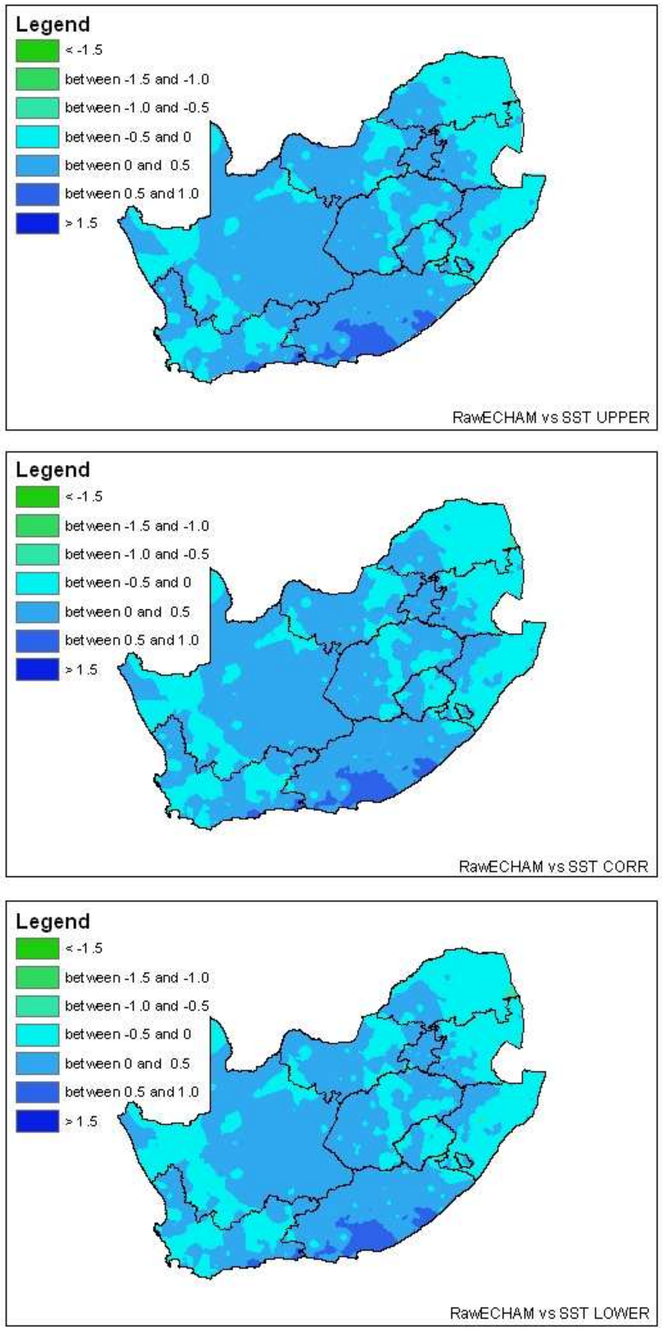

Figure 4.17. Correlation differences between the raw ECHAM4.5 (4 ensemble members) and the baseline model (SST as predictors) over the 10-year test period of 1991/92 to 2000/01. The top panel shows the upper limit and the bottom panel the lower limit of the 95% significance level.

The spatial distribution in simulation skill has been demonstrated above. Figure 4.18 shows the performance of the simulation methods over the 10-year test period averaged over the 963 stations. The time series in the figure are standardized departures. Correlation values associated with the MOS and raw ECHAM4.5 systems are high and between 0.4 and 0.5, with the correlation associated with the SST baseline model of 0.2, followed by the nested system of only 0.1. As with the simulations for regional rainfall, simulated anomalies are generally overestimated during the El Niño season of 1997/97 and the La Niña season of 1998/99, while the wet conditions during 1995/96 are underestimated. Notwithstanding the poor temporal skill of the GCM-RCM system (0.1), simulation produced with the nested approach was skilful during the wet year of 1995/96 when the other systems failed to capture the wet anomaly. With the exception of the nested system, the rainfall during the 1999/2000 La Niña season is skillfully simulated by most of the systems, especially by the ECHAM4.5-MOS system.

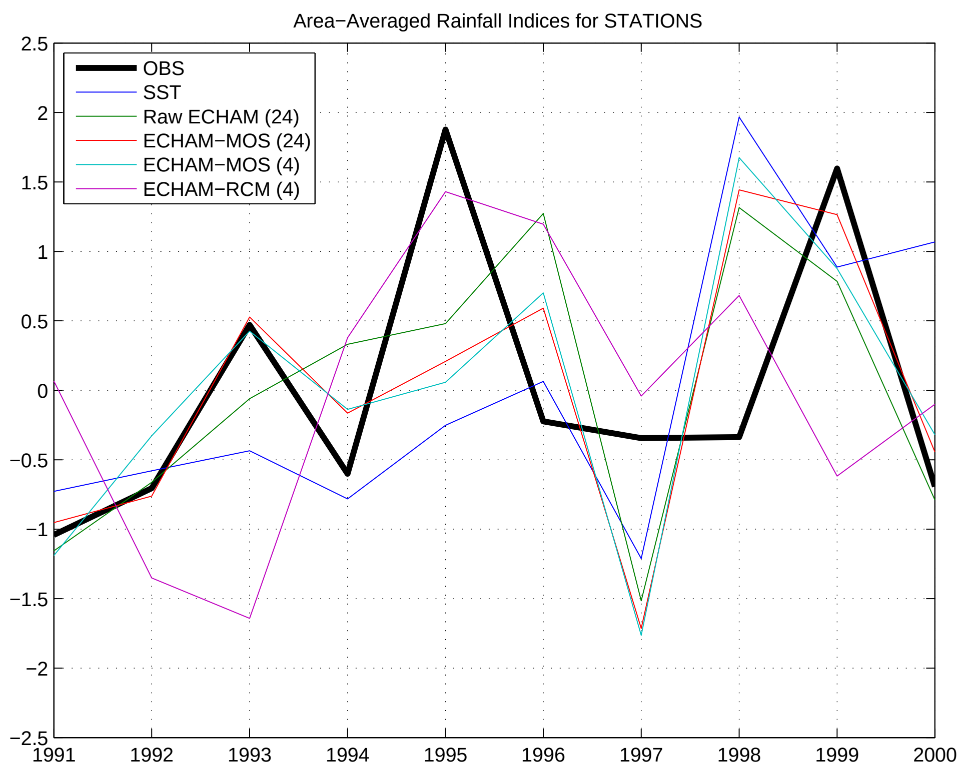

Figure 4.18. Regional area-averaged simulation performances over the 10-year test period.

4.2.3. Post-processing nested simulations

The advantages of statistically correcting dynamical model output to station level have been demonstrated in Section 4.2.2. Figure 4.19 shows the result of doing a 1-year-out cross-validation procedure over the 10 years relating the simulated 850 hPa geopotential height field of the ECHAM4.5-RegCM3 system to station rainfall. Area-averaged indices are again calculated and shown in the figure. The MOS process improves the correlation value from 0.1 to 0.5. However, a period longer than 10 years is required to test the robustness of the prediction equations.

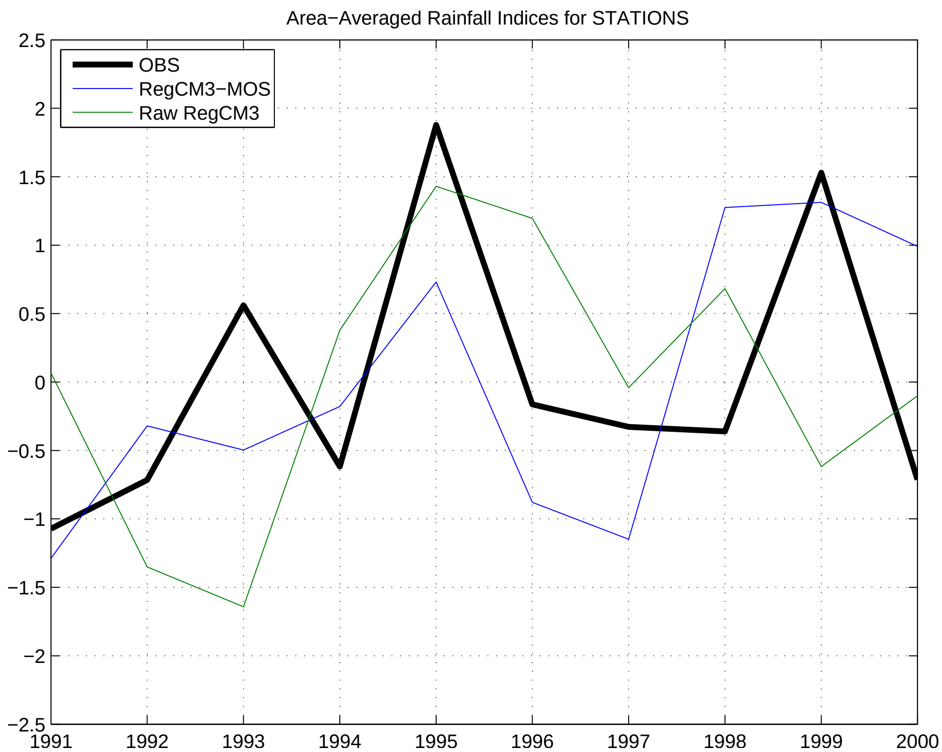

Figure 4.19. Station area-average simulation performance of the raw ECHAM4.5-RegCM3 system and the ECHAM4.5-RegCM3-MOS system.

4.2.4. GCM vs. NCEP nesting

The RegCM3 is also nested in the large-scale driving fields obtained from the NCEP reanalysis data set and its simulations skill compared with the skill from the GCM-RCM system. The results presented as station area-averaged values are shown in Figure 4.20. In contrast to the nested results obtained from doing a regional average, both the correlations between the observed rainfall and the nested simulations are low, even though the NCEP-RegCM3 system is associated with a higher correlation value (0.1 for ECHAM-RegCM3 and 0.3 for NCEP-RegCM3).

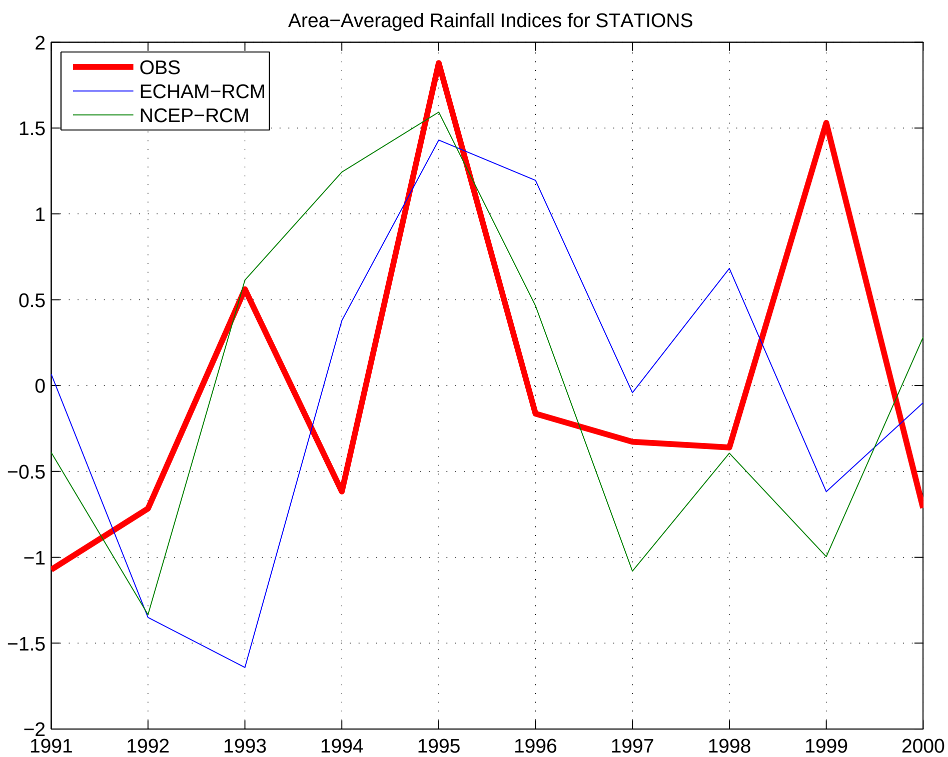

Figure 4.20. Station area-average simulation performance of the ECHAM4.5-RegCM3 system and the NCEP-RegCM3 system.

The correlation differences suggest that the NCEP-RegCM3 system is only slightly outperforming the ECHAM4.5-RegCM3 system. Figure 4.21 provide further evidence that the two systems are associated with about the same amount of skill on a station level since correlation differences per station vary about equally between -0.5 and 0.5 (Figure 4.22).

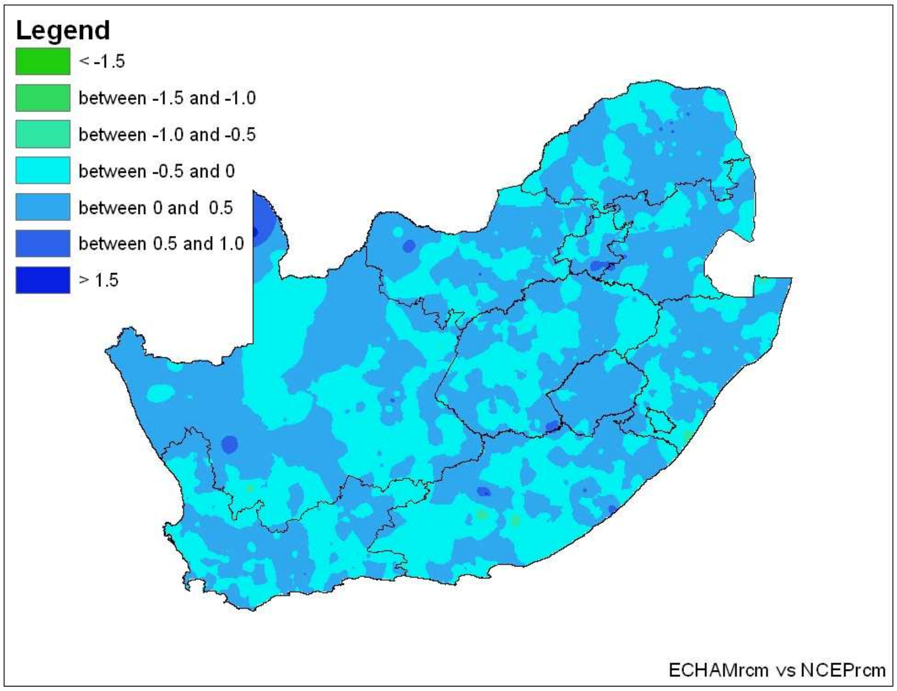

Figure 4.21. Correlation differences between the ECHAM4.5-RegCM3 and the NCEP-RegCM3 over the 10-year test period of 1991/92 to 2000/01.

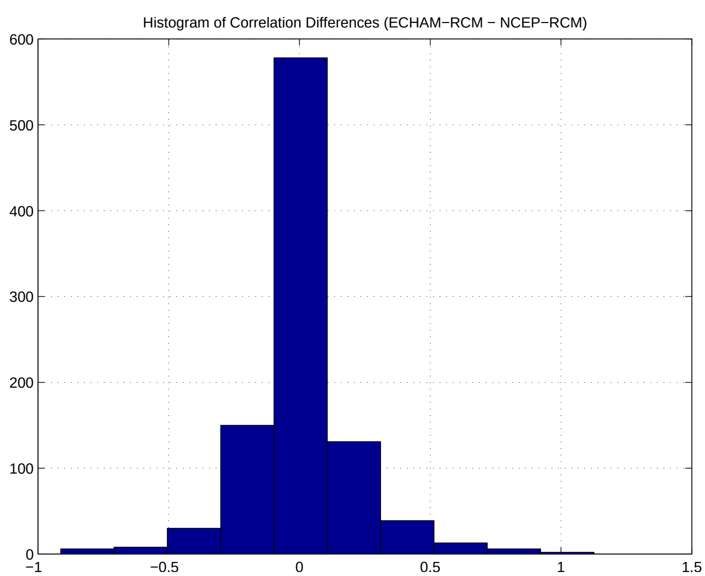

Figure 4.22. Histogram of correlation differences between the ECHAM-RegCM3 system and the NCEP-RegCM3 system.

4.3. Synopsis

Simulation skill at station level has been demonstrated over the 10-year test period (1991/92 to 2000/01). Although this is a short period, subsequently making it difficult to unequivocally state which simulation method is better than the other, useful conclusions can be drawn from the analyses. The following have been demonstrated:

1. On a station level poor skill is associated with the ECHAM4.5-RegCM3 and NCEP-RegCM3 systems, and they produce about equally skilful simulations;
2. For the larger part of the country, the nested systems are outperformed by the raw GCM and GCM-MOS systems, but are strong competitors compared to the baseline system, excluding the north-eastern parts of the country where SSTs provide good simulation skill;
3. For the larger part of the country, the GCM-MOS system outperforms the raw GCM and baseline simulations, and the raw GCM system outperforms the baseline system except over the north-eastern parts; and,
4. The full ensemble GCM and GCM-MOS simulations produce skill levels which are higher than the 4-member simulations, reemphasizing the previous finding that increased ensemble size improves on model simulations; therefore, nested-system skill levels may be enhanced with increasing ensemble size.

The potential for using statistical downscaling methods for modelling South African seasonal regional rainfall variability has been demonstrated. Skill may be further improved with larger ensemble sizes for both types of downscaling approaches and through statistical post-processing of nested model output.

CHAPTER 5:
THE INTERNAL VARIABILITY OF THE RegCM3

5.1. Introduction

General Circulation Models (GCMs) are used at several centres as part of a two tier system for making seasonal climate forecasts up to several seasons in advance. The SSTs are predicted first, and these are then used as surface boundary conditions for ensembles of predictions with GCMs (Robertson et al, 2004). GCMs simulate precipitation and temperature and other atmospheric variables, with a resolution of about 300 km across the globe. It is necessary that multiple realizations are made for each model to make the predictions more robust and to quantify the uncertainty (Fenessy and Shukla, 2000; AMS, 2001; Shukla et al, 2000). Dynamical downscaling can be used to produce high resolution simulations at a lower cost than that required for a GCM with the same resolution (Giorgi, 1990). An RCM is nested within a GCM or global reanalyses which provide the required large-scale conditions (the initial conditions (ICs) and the time dependant lateral boundary conditions (LBCs)) (Fennessy and Shukla, 2000; Giorgi, 1990).

Tropical flow patterns and rainfall are strongly determined by the slow evolution of surface conditions, most notably SSTs. However, the natural internal atmospheric variability of the extratropical atmosphere limits the impact of tropical SST forcing. The internal variability of the models is central to the question of the predictability of the atmosphere. In operational forecasting, multiple realisations are made using the GCM, due to non-linearities in the GCM (Giorgi and Bi, 2000). GCM solutions started with initial conditions that are slightly different from one another will diverge substantially after a few days of simulations. The solutions will diverge from one another as a result of the internal variability of the GCM. The differences among the ensemble members give the forecasts some measure of the likelihood that a particular seasonal climate state will be below, in, or above the normal interval (AMS, 2001).

In regional climate modeling an RCM is nested within a GCM which provides the ICs and the time dependent LBCs. The lateral boundary forcing limits the degrees of freedom of RCMs, so that an RCM climatology will not strongly diverge from the forcing fields (Giorgi and Bi, 2000). The RCM's physics and dynamics are also non-linear and hence, although they are restricted by the boundary forcing, they are expected to exhibit a certain level of the internal variability. If an RCM is nested within a GCM the solutions that are obtained are a function of the internal variability of GCM as well as of the RCM. It is therefore necessary to investigate the amount of variability introduced to a nested system's solution by the RCM's internal variability. The question is central to seasonal forecasting using an RCM because it has to be established whether or not it is necessary to produce multiple realisations to quantify the uncertainty associated with the internal variability of the RCM as it is done for the GCMs in forecasting applications. This part of the study is aimed at investigating the variability in the solutions caused by non-linearities in the GCM as well as in the RCM. The study then investigates the amount of variability which is introduced by the RCM.

5.2. Method

The GCM used in the study is the ECHAM4.5 and this model is used because it was found to outperform four other GCMs over southern Africa in previous studies (Landman and Goddard, 2003). The GCM integrations used in the study are made at the International Research Institute for Climate and Society (IRI). Four ECHAM4.5 solutions obtained through perturbing the wind fields are used to force the RegCM3. The analysis of the generated data gives the internal variability of the ECHAM4.5 and the RegCM3. The analysis will give the internal variability of the GCM and the RCM because the solutions will be different from one another on the basis of initial conditions supplied to the GCM being different from each other. The RCMs are non-linear and therefore their internal variability also influences the solutions. The simulations are made over a 10 year period and for December-February (DJF).

To investigate the amount of variability in the nested system solutions that is introduced by the internal variability of the RegCM3, the RegCM3 is nested within one realisation of the GCM. Four solutions of the RegCM3 are then generated through initialising the RegCM3 on different days using a single realisation from the ECHAM4.5. The difference between the RCM solutions is therefore caused only by the different initial conditions supplied to the RCM. The LBCs and surface conditions are constant for each year. The difference among the RCM solutions gives the internal variability of the RegCM3. To make sure that the results obtained using a single realisation from the ECHAM4.5 are consistent for all the other realisations one more realisation is used and the same procedure is followed. For this study only two seasons that were highly anomalous are studied, 1992/92 (Figure 5.1) and 1995/96 (Figure 5.2).

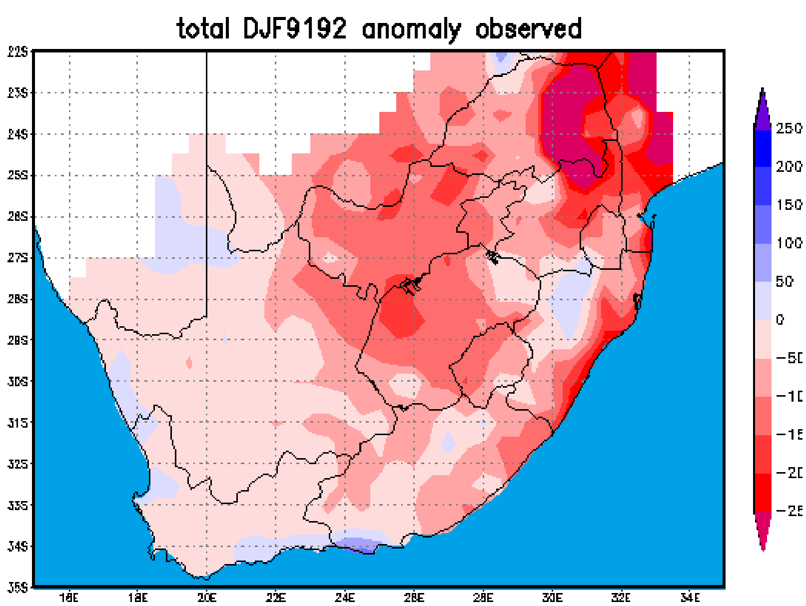

Figure 5.1. The total DJF 1991/92 rainfall anomaly based on the ten years average from 1991/92 to 2000/2001.

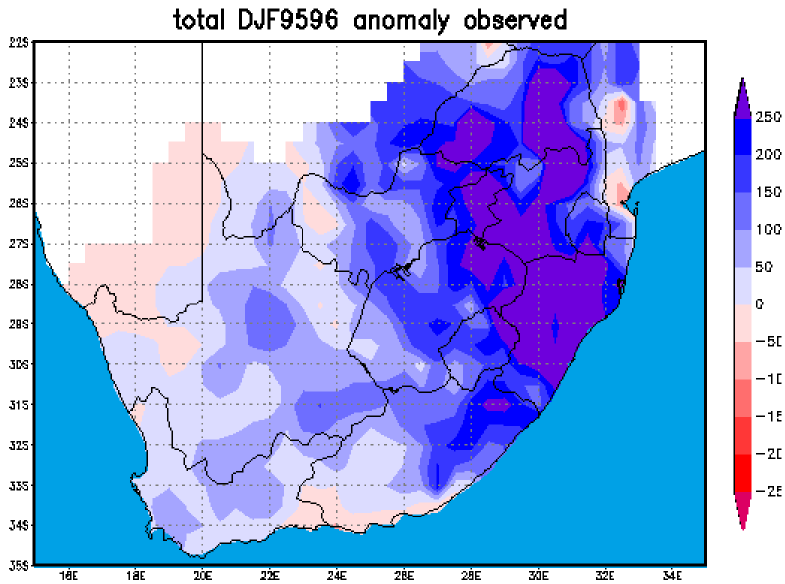

Figure 5.2. The total DJF 1995/96 rainfall anomaly based on the ten years average from 1991/92 to 200/2001

5.3. Results

5.3.1. The internal variability of both the GCM and the RCM

The SST forced variance, the internal dynamics variance and the total variance (Shukla et al, 2000) are calculated using 10 years of data as simulated by the RegCM3 forced with four ensemble members from the ECHAM4.5 GCM. The variance of the ensemble average seasonal means among all the years is referred to as the SST forced variance or signal. The variance within each ensemble averaged for all the years is referred to as the internal dynamics variance or noise. The total variance is the sum of the signal plus noise variances.

5.3.2. Variances

The most surface pressure variance occurs in the Indian Ocean and also South of the continent (Figure 5.3). The simulated areas of maximum pressure variance correspond with the observed variance from the NCEP reanalyses (Figure 5.3; Figure 5.4). The high variability south of the country is caused by the cold fronts that have centres of low pressure and the high pressure cells that usually ridge south of the country. The high variability in the Indian Ocean is due to the transition from the Indian Ocean highs and the tropical cyclones which usually occur over the region (Tyson and Preston-Whyte, 2000). The areas of the simulated maximum temperature variance correspond with the observed. The simulated and observed temperature variability is small over the oceans because SSTs are slowly evolving and as a result the temperatures variations are not as high as over land. The simulated and observed areas of maximum rainfall variance do not correspond (Figure 5.5; Figure 5.6; Figure 5.7). The observed highest variability occurs over the coast of Mozambique while in the simulations it occurs on the eastern side of Madagascar, north of Madagascar and some areas over tropical Africa. The area over tropical Africa where the simulated variability is high is observed to have very little variability. This may not be a true reflection of the variance in the region due to a lack of observational data. High simulated magnitudes of variance also occur along the boundaries of the model due to spurious rainfall that is caused by the inconsistencies between the LBCs and the model domain's internal climatology.

The variances that are calculated are for temperature, surface pressure and rainfall. The SST forced variance and the internal model dynamics variance are calculated for each of the three variables. In all the instances the variability associated with the internal variability of the models is higher than the SST forced variance (Figure 5.5; Figure 5.6). The results suggest that the variability of the ensemble members in a particular season exceeds the variability of the ensemble average over the 10 year period. To further investigate the simulated rainfall variability, analyses are made over South Africa using eight homogeneous regions.

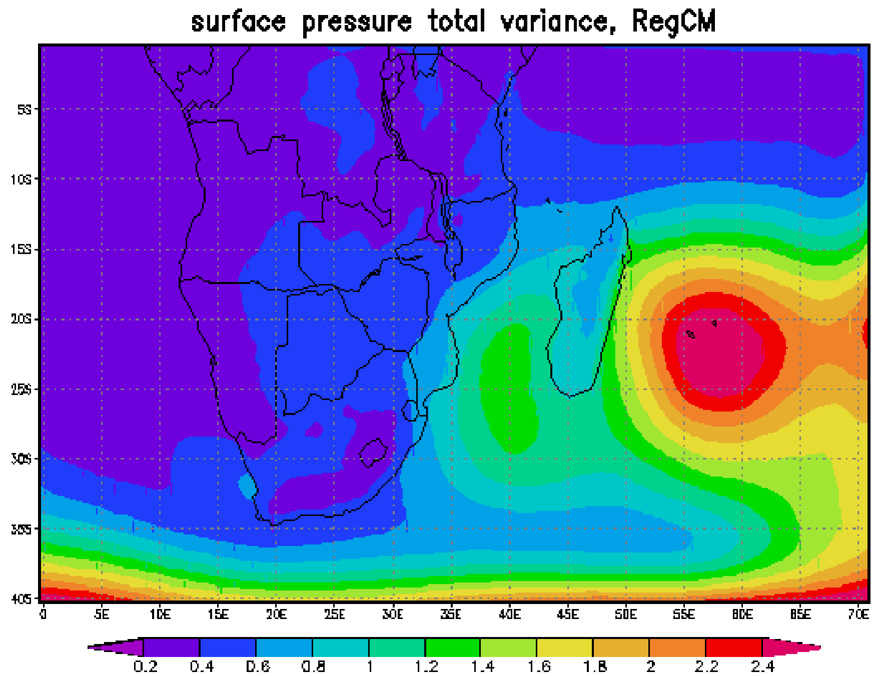

Figure 5.3. The total surface pressure variance for 10 DJF seasons with 4 ensemble members

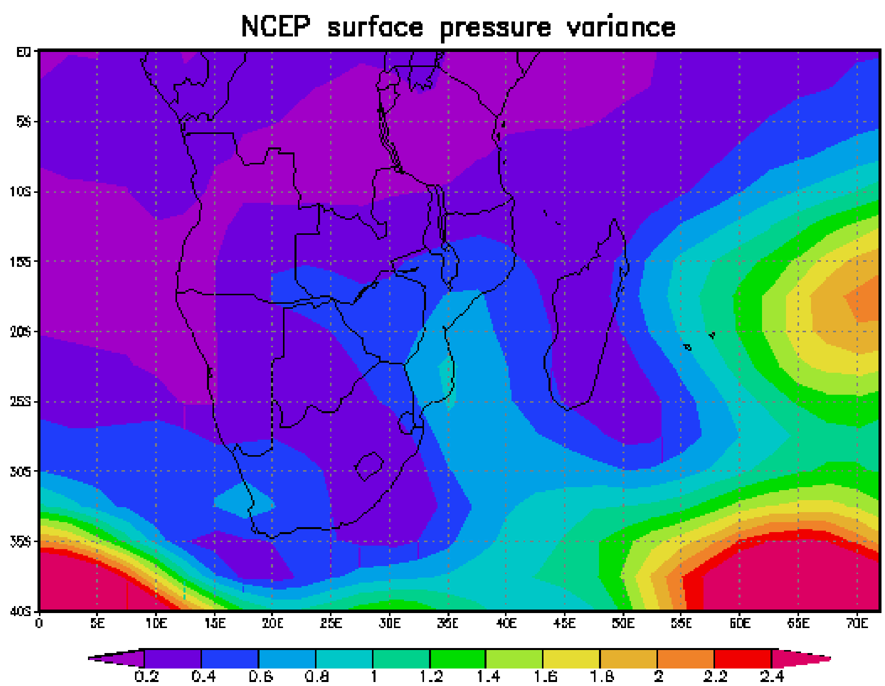

Figure 5.4. The surface pressure total variance as calculated from the NCEP reanalysis for the DJF season from 1991/92 to 2000/2001.

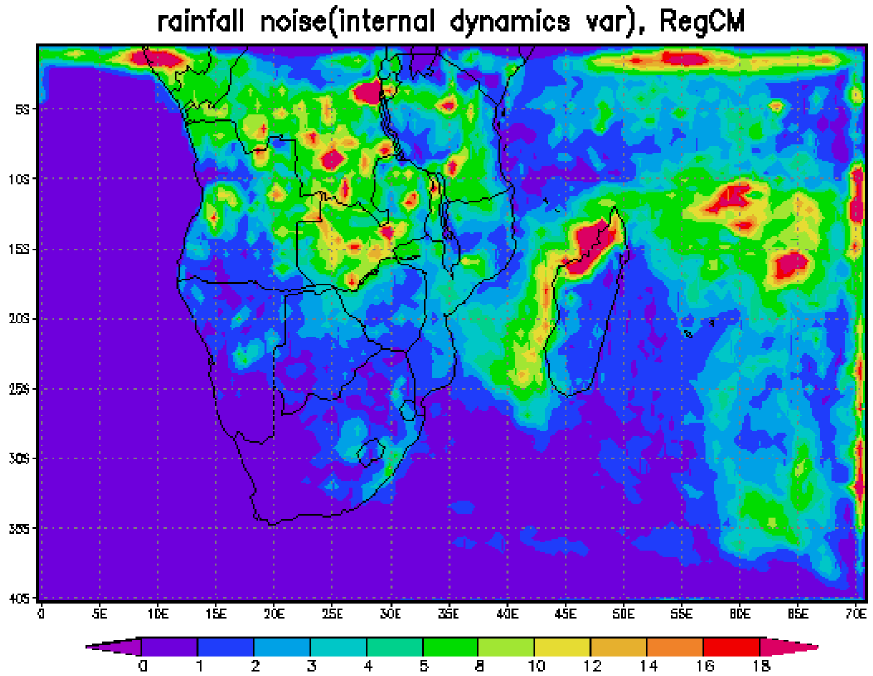

Figure 5.5. The rainfall internal dynamics variance for 10 DJF seasons with 4 ensemble members

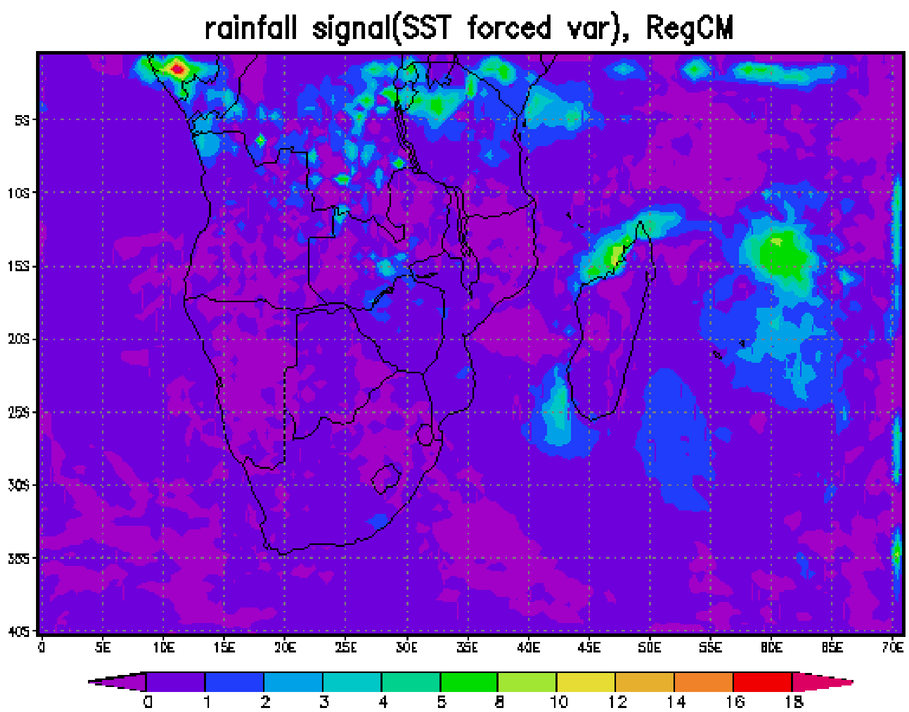

Figure 5.6. The SST forced rainfall variance for 10 DJF seasons with 4 ensemble members

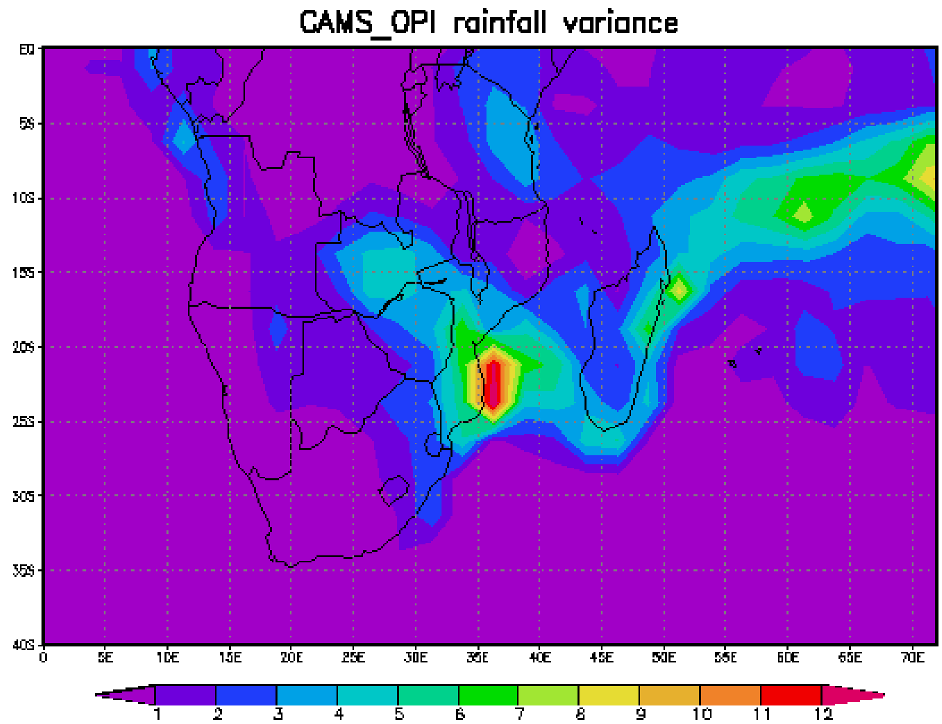

Figure 5.7. The monthly rainfall variance as calculated from CAMS_OPI for the DJF season from 1991/92 to 2000/2001.

5.3.3. The homogeneous regions

Model data of the gridpoints within each of the eight regions are used to construct rainfall time series that can be compared with observed time series. The total rainfall for each region for the four ensemble members is plotted on a time series together with the ensemble average and the observed rainfall over a 10 year period (Figure 5.8; Figure 5.9; Figure 5.10). The ensemble average exhibits a small variance because of the high variability of the ensemble members in different seasons. The ensemble members are more in phase over the central parts of the country (Figure 5.9), with high variability over the regions towards the eastern part of the country (Figure 5.10). The model solutions correspond with the observations mostly over the central part of South Africa with the least correspondence over the east (Figure 5.9). The model overestimates rainfall over the eastern coast (Figure 5.8). The rainfall overestimation is a feature that may be attributable to the steep topographic gradients in the area.

Pal et al (2005) found that the RegCM3 tends to overestimate rainfall in areas of steep topographic gradients in South America, Asia and in West Africa. When the anomalies are analysed the model still performs better in the central and western parts than in the eastern part of South Africa. The skill of statistical downscaling models was also found to be higher in the central interior of South Africa in the previous studies (Landman and Tennant, 2000). The area where the models seem to be performing the best has the highest correlation with the Nino 3.4 SSTs (Kruger, 1998).

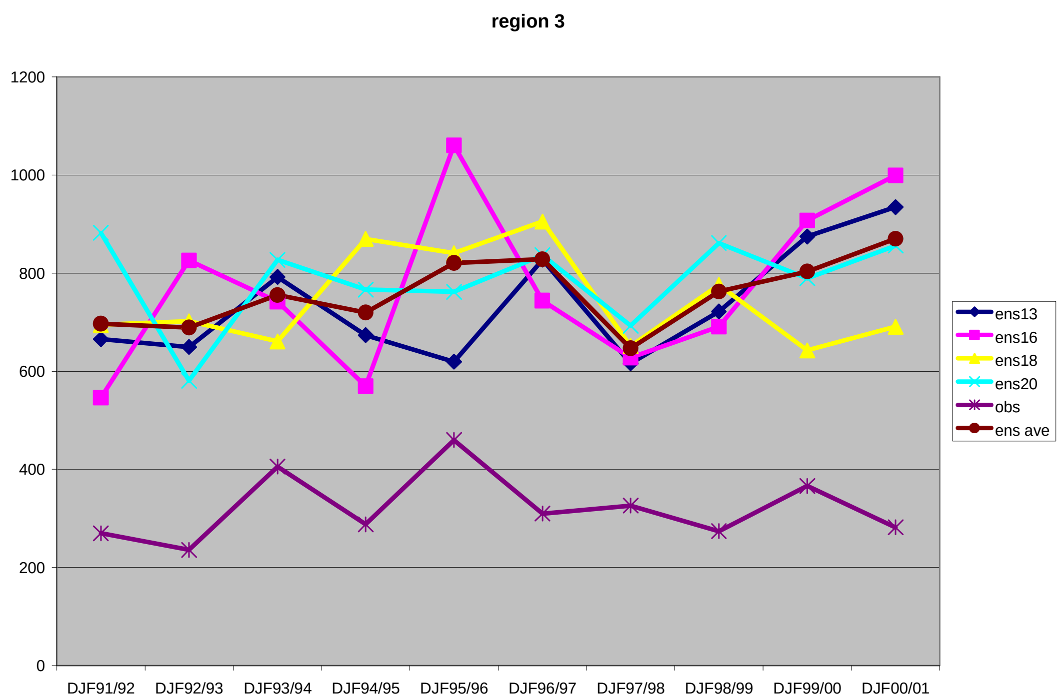

Figure 5.8. The total 10 year DJF rainfall for region 3 for the four ensemble members, the ensemble average and the observations.

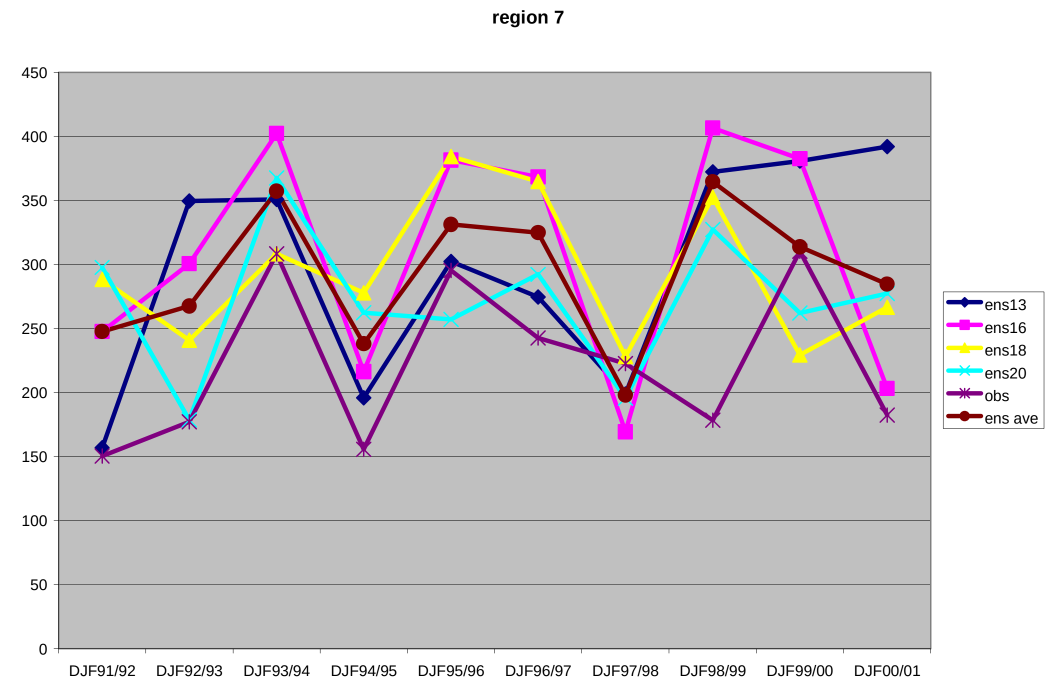

Figure 5.9. The total 10 year DJF rainfall for region 7 for the four ensemble members, the ensemble average and the observations.

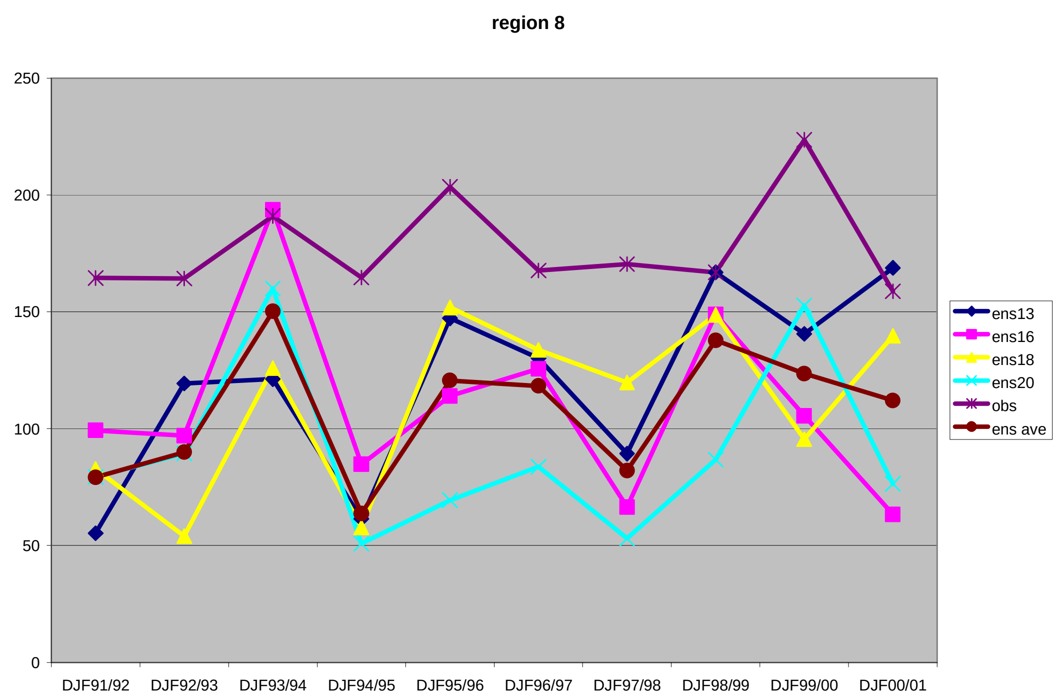

Figure 5.10. The total 10 year DJF rainfall for region 8 for the four ensemble members, the ensemble average and the observations.

The above simulations are different from each other due to the internal variability of both the GCM and the RCM. In seasonal prediction it has already been established that multiple realizations should be made in sensitivity studies as well as in the operational forecasting to quantify the uncertainty of the GCM non-linearities. It has, however, not been established yet whether or not multiple realisations should be made to quantify the uncertainty associated with the RCM’s internal variability.

5.3.4. The internal variability of the RegCM3

This part of the study is aimed to investigate the amount of variability that is introduced by the RCM. Two highly anomalous seasons are analyzed and the model’s internal variability based on the two seasons is discussed. The four ensemble members obtained by initializing the ECHAM4.5 on different days and four ensemble members obtained by initializing the RegCM on different days are analyzed. The former gives the measure of the internal variability of the GCM and the RCM while the latter gives the internal variability of the RCM. The model solutions obtained by initialising the GCM on different days are quite different from each other (Figure 5.11; Figure 5.12) while those obtained by initialising the RegCM3 on different days are generally similar (Figure 5.11; Figure 5.14). The results suggest that the variability that is found amongst the ensemble members that are generated by initializing the GCM on different days is due to more non-linearities in the GCMs than to the RCM’s internal variability.

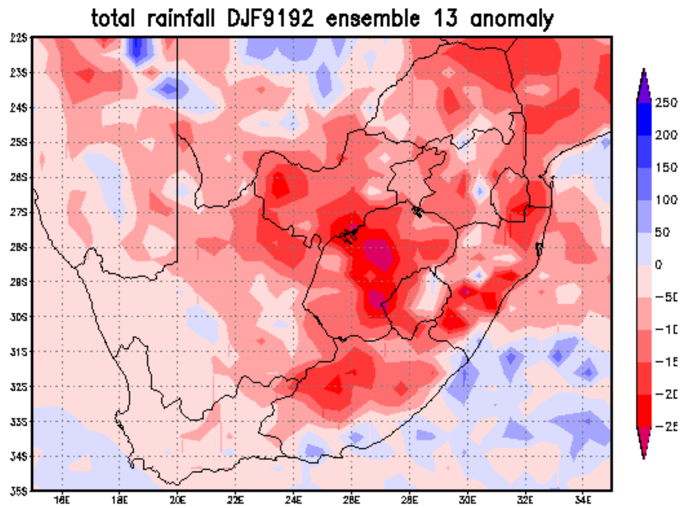

Figure 5.11. The DJF 1991/92 Ensemble 13 total rainfall anomaly.

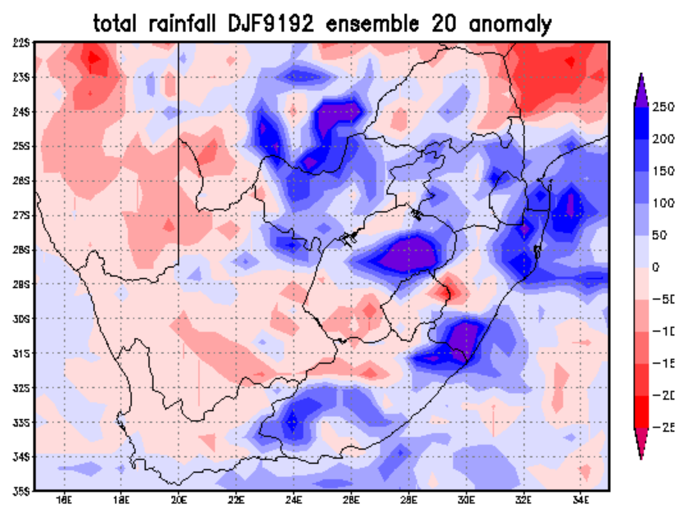

Figure 5.12. The DJF 1991/92 Ensemble 20 total rainfall anomaly

The model captured the general direction of the rainfall anomalies in the two seasons. The anomalies associated with the ensemble averages are quite small when compared to the observations and also when compared to the individual ensemble member anomalies. This is because the ensemble member simulations are very different from each other and therefore averaging them and then subtracting the ensemble average over the 10 years does not give big anomalies. Ensemble member 13 performs the best for the 1991/92 season (Figure 5.1; Figure 5.11) and in 1995/96 the situation is reversed (not shown).

Ensemble 20 performs the worst in the 1991/92 season (Figure 5.1; Figure 5.12). In both seasons the ensemble average captures the general direction of the observed anomaly. These results show that multiple realizations contributed to reduce the uncertainty in the forecasts. In addition, most of the variability that is found in the ensemble members obtained from a nested system is due to non-linearities in the GCM.

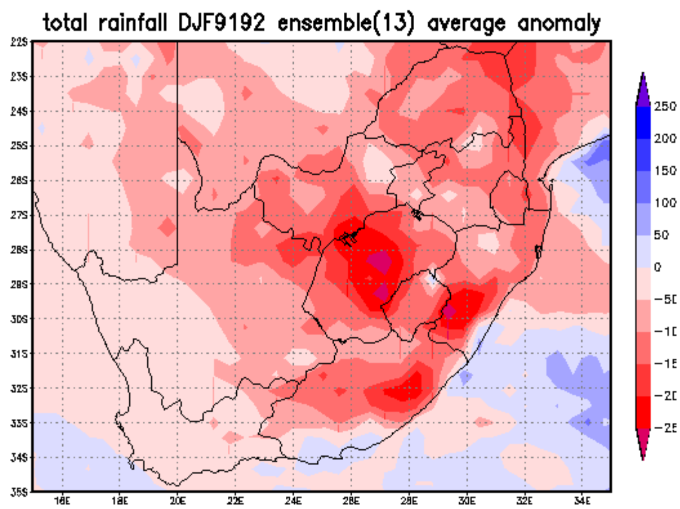

Figure 5.13. The DJF 1991/92 Ensemble 13 ensemble average total rainfall anomaly.

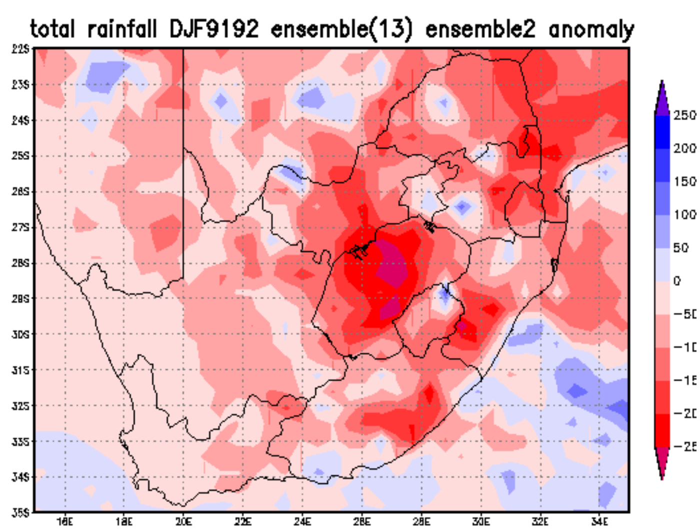

Figure 5.14. The DJF 1991/92 Ensemble 13 ensemble 2 total rainfall anomaly.

5.4. Synopsis

The lateral boundary forcing provided by a GCM limits the degrees of freedom of RCMs, so that the RCM climatology will not strongly diverge from the forcing fields. The RCMs are non-linear models and as a result, although they are restricted at the boundaries, they are expected to exhibit a certain level of the internal variability of the system. It is therefore expected that in a nested system where a GCM is used to provide LBCs, the nested system solutions will be functions of the internal variability of both the GCM and the RCM. In forecasting multiple realizations are already made to quantify the uncertainty associated with the GCM's non-linearities. The study is aimed to investigate whether or not in regional climate modelling multiple realizations need to be made to quantify the uncertainty associated with the non-linearities in the RCM. To do that the contribution of the RCM's non-linearities towards the variability of ensemble members is analyzed.

High variability is found with the ensemble members that are functions of the non-linearities of the GCMs and the RCMs. However, simulations of the ensemble members associated with the non-linearities in the RCM are almost similar to one another. This result suggests that the variability that is observed on the original four ensemble members is more a result of the internal variability of the GCM than it is of the internal variability of the RCM. The RCM's internal variability, therefore, makes a small contribution towards the variability of the ensemble members, suggesting that the LBCs play a more important role than do the ICs. The results suggest that seasonal forecasts do not require multiple realisations to cater for the internal variability of the RCM.

CHAPTER 6:
CONCLUSIONS AND RECOMMENDATIONS

The study has investigated the performance of a number of simulation systems (no forecast lead-time) of varying complexity. These systems' performance is tested for the December-January-February (DJF) rainfall for both homogeneous regions and for 963 stations, and compared with each other over a 10-year test period from 1991/92 to 2000/01. Although this test period is too short to unequivocally demonstrate which simulation method is the best, the following conclusions have been drawn from the analyses:

1. For the most part the simulation methods outscore the baseline method that uses sea-surface temperature (SST) anomalies to simulate rainfall;
2. There are advantages in statistically post-processing output from general circulation models (GCMs) as well as output from regional climate models (RCMs);
3. Simulation skill should improve with an increased number of ensemble members; this also holds true for nested systems that were generally outscored by the GCM and GCM-MOS systems presented here;
4. Since multiple realizations are not required to describe the internal variability of the RCM, increasing the ensemble size of the nested system would mainly contribute to probabilistic forecast skill.

The *potential* for using dynamical and statistical downscaling methods and their combination for forecasting South African seasonal regional rainfall variability is an operational environment has been demonstrated. In addition to expanding on the number of ensemble members, the test period of 10 years should be increased in order to test the robustness of the results presented here. An increased ensemble size can also be used to test the probabilistic skill levels of these systems and how they can be used in an operational seasonal forecasting environment that demands a description of forecast uncertainties.

REFERENCES

AMS statement, 2001: Seasonal to Interannual climate prediction. *Bulletin of American Meteorological Society,* **82,** 701-703.

Anthes, R. A., Y. –H. Kuo, E. –Y. Hsie, S. Low-Nam, and T. W. Bettge, 1989: Estimation of skill and uncertainty in regional numerical models. *Quarterly Journal of the Royal Meteorological Society*, **115**, 763-806.

Barnston, A. G., 1994: Linear statistical short-term climate predictive skill in the Northern Hemisphere. *Journal of Climate*, **7**, 1513-1564.

Barnett, T. P., and R. W. Preisendorfer, 1987: Origins and levels of monthly and seasonal forecast skill for United States air temperature determined by canonical correlation analysis, *Monthly Weather Review*, **11**5, 1825-1850.

Chouinard, C., J. Mailhot, H. L. Mitchell, A. Staniford, and T. Hogue, 1994: The Canadian regional data assimilation system: Operational and research applications. *Monthly Weather Review*, **122**, 1306-1325.

Cook, C., C. J. C. Reason, and B. C. Hewiston, 2004: Wet and dry spells within particularly wet and dry summers in the South African summer rainfall region. *Climate Research*, **26**, 17-31.

D'Abreton, P.C. and J.A. Lindesay, 1992: Water vapour transport over southern Africa during wet and dry early and late summer months. *International Journal of Climatology*, **13**, 151-170.

Druyan, L. M., M. Fulakeza, P. Lonergan and M. Saloum, 2000: A regional model study of synoptic features over West Africa. *Monthly Weather Review*. **129**, 1564-1577.

Fennessy, M. J., and J. Shukla, 2000: Seasonal prediction over North America with a regional model nested in a global model. *Journal of Climate,* **13**, 2605–2627.

Giorgi, F., 1990: Simulation of regional climate using a limited area model nested in a general circulation model. *Journal of Climate*, **3**, 941–964.

Giorgi, F., and X. Bi, 2000: A study of the internal variability of a regional climate model. *Journal of Geophysical Research*, **105**, 29503-29521.

Giorgi, F., and L. O. Mearns, 1999: Introduction to special section: regional climate modelling revisited. *Journal of Geophysical Research*, **104**, 6335-6351

Giorgi, F., M. R. Marinucci, G. T. Bates, 1993a: Development of a second-generation regional climate model (RegCM2). Part I: Boundary-layer and radiative transfer processes. *Monthly Weather Review*, **121**, 2794–2813.

Giorgi, F., M. R. Marinucci, G. T. Bates, and G. De Canio, 1993b: Development of a second-generation regional climate model (RegCM2). Part II: Convective processes and assimilation of lateral boundary conditions. *Monthly Weather Review*, **121**, 2814–2832.

Giorgi, F., L. O. Mearns, C. Shields, L. and Mayer, 1996: A regional model study of the importance of local versus remote controls of the 1988 drought and the 1993 flood over the central United States. *Journal of Climate*, **9**, 1150-1162.

Goddard L., S. J. Mason, S. E. Zebiak, C. F. Ropelewski, R. Basher, and M. A. Cane, 2000: Current approaches to seasonal-to-interannual climate predictions. *International Journal of Climatology*, **21**, 1111-1152.

Gong, X., A. G. Barnston, M. N. Ward, 2003: The effect of spatial aggregation on the skill of seasonal precipitation forecasts. *Journal of Climate*, **16**, 3059-3071.

Grell, G. 1993: Prognostic evaluation of assumptions used by cumulus parameterization. *Monthly Weather Review*, **121**, 764-787.

Grell, G. A., J. Dudhia, and D. R. Stauffer, D. R. 1994: A description of the fifth-generation penn state/NCAR mesoscale model (MM5), National Center for Atmospheric Research Technical report. TN-398+STR, 121pp.

Hoffman, R. N. and E. Kalnay, 1983: Lagged average forecasting, an alternative to Monte Carlo forecasting. *Tellus*, **35A**, 100-118.

Jackson, J. E., 1991: *A User's Guide to Principal Components*, Wiley, New York, p. 569.

Joubert, A. M., and B. C. Hewitson, 1997: Simulating present and future climates of southern Africa using general circulation models. *Progress in Physical Geography*, **21**, 51-78.

Joubert, A. M., J. J. Katzfey, J. L., McGregor, and K. C. Nguyen, 1999: Simulating midsummer climate over southern Africa using a nested regional climate model. *Journal of Geophysical Research*, **104**, 19015-19025.

Kiehl, J., J. Hack, G. Bonan, B. Boville, B. Breigleb, D. Williamson, and P. Rasch, 1996: Description of the NCAR community climate model (CCM3), *National*

Centre for Atmospheric Research (NCAR) Technical Report. TN-420 + STR, 152 pp.

Kim J., N. L. Miller, J. D. Farrara, and S. Hong, 2000: A seasonal precipitation and stream flow hindcast and prediction study in the western United States during the 1997/1998 winter season using a dynamic downscaling dystem. *Journal of Hydrometeorology,* **1,** 311-329.

Krishnamurti, T. N., C. M. Kishtawal, Z. Zang, T. LaRow, D. Bachiochi, E. Williford, S. Gadgil, and S. Surendran, 2000: Multimodel ensemble forecasts for weather and seasonal climate. *Journal of Climate*, **13**, 4196-4216.

Kruger, AC, 1998: The influence of the decadal-scale variability of summer rainfall on the impact of El Niño and La Niña Events in South Africa. *International Journal of Climatology*. **19,** 59-68.

Landman, W. A., and L. Goddard, 2002: Statistical recalibration of GCM forecasts over southern Africa using model output statistics. *Journal of Climate*, **15**, 2038-2055.

Landman, W. A., and L. Goddard, 2003: Model output statistics applied to multi-model ensemble forecasts for southern Africa. *Proceedings of the 7th International Conference on Southern Hemisphere Meteorology and Oceanography*. American Meteorological Society, 249-250.

Landman, W. A., and S. J. Mason, 1999: Operational long-lead prediction of South African rainfall using canonical correlation analysis. *International Journal of Climatology*, **19**, 1073-1090.

Landman, W. A. and Tennant, W. J. 2000. Statistical downscaling of monthly forecasts. *International Journal of Climatology*, **20**, 1521-1532.

Landman, W. A., A. Seth, and S. J. Camargo, 2005: The effect of regional climate model domain choice on the simulation of tropical cyclone-like vortices in the southwestern Indian Ocean. *Journal of Climate*, **10**, 1263-1274.

Landman, W. A., S. J. Mason, P. D. Tyson, and W. J. Tennant, 2001a. Retro-active skill of multi-tiered forecasts of summer rainfall over southern Africa. *International Journal of Climatology*, **21**, 1-19.

Landman, W. A., S. J. Mason, P. D. Tyson, and W. J. Tennant, 2001b: Statistical downscaling of GCM simulations to streamflow. *Journal of Hydrology*, **252**, 221-236.

Mason, S. J., 1998: Seasonal forecasting of South African rainfall using a non-linear discriminant analysis model. *International Journal of Climatology*, **18**, 147-164.

Mason, S. J., and A. M. Joubert, 1997: Simulating changes in extreme rainfall over southern Africa. *International Journal of Climatology*, **17**, 291-301.

Mason, S. J., and M. R. Jury, 1997: Climate variability and change over southern Africa: a reflection on underlying processes. *Progress in Physical Geography*, **21**, 23-50.

Pal, J., E. Small, and E. Eltahir, 2000: Simulation of regional-scale water and energy budgets: Representation of subgrid cloud and precipitation processes within RegCM, *Journal of Geophysical Research-Atmospheres*, **105**, 29579-29594.

Pal J.S., F. Giorgi, X. BI, N. Elguindi, F. Solmon, X, Gao, R. Francisco, A. Zakey, J. Winter, M. Ashfaq, F.S. Syed, J.L. Bell, N.S. Diffenbaugh, J. Karmacharya, A.

Konare, D. Martinez, R.P. da Rocha, L.C. Sloan and A. Steiner, 2005: The ICTP RegCM3 and RegCNET: Regional Climate Modelling for the Developing World. *Submitted to the Bulletin of the American Meteorological Society*,39 pp.

Pan, Z., E. Tackle, W. Gutowski, and R. Turner, 1998: Long simulation of regional simulation of regional climate as a sequence of short segments. *Monthly Weather Review*. **127**, 308-321

Qian J. –H. A. Seth, and S. Zebiak, 2003: Reinitialised versus continuous simulations for regional climate downscaling. *Monthly Weather Review*, **131**, 2857-2873.

Reason, C. J. C., 2001: Subtropical Indian Ocean SST dipole events and southern African rainfall, *Geophysical Research Letters,* **28***,* 2225-2227.

Reynolds, R. W., and T. M. Smith, 1994: Improved global sea surface temperature analyses using optimum interpolation. *Journal of Climate,* **7**, 929-948.

Roeckner, E., and Coauthors, 1996: *The atmospheric general circulation model ECHAM4: Model description and simulation of present-day climate*. Max-Planck-Institüt für Meteorologie Report 218, p. 90.

Robertson, A. W., U. Lall, S. E. Zebiak, and L. Goddard, 2004: Improved Combination of Multiple Atmospheric GCM Ensembles for Seasonal Prediction. *Monthly Weather review*, **132**, 2732-2744.

Seth, A., and F. Giorgi, 1998: The effects of domain choice on summer precipitation simulation and sensitivity in a regional climate model. *Journal of Climate*, **11**, 2698-2712.

Shepard, D., 1968: A two-dimensional interpolation function for irregularly-spaced data. *Proceedings of the 23rd National Conference ACM, ACM*, 517-524.

Shongwe, M. E., W. A. Landman, and S. J. Mason, 2006: Performance of recalibration systems of GCM forecasts for southern Africa. *International Journal of Climatology*, in press.

Shukla, J., J. Anderson, D. Baumhefner, D. Baumhefner, C. Brankovic, Y. Chang, E. Kalnay, L.Marx, T. Palmer, P. Paolino, J. PLoshay, S. Schubert, D. Straus, M. Suarez, and J. Tribbia, 2000: *Dynamical Seasonal Prediction. Bulletin of the American Meteorological Society*, **81**, 2593-2606.

Smith, T. M., R. W. Reynolds, R. E. Livezey, and D. C. Stokes, 1996: Reconstruction of historical sea surface temperatures using empirical orthogonal functions, *Journal of Climate,* **9**, 1403-1420.

Taylor, A. A., and L. M. Leslie, 2005: A single-station approach to model output statistics temperature forecast error assessment. *Weather and Forecasting*, **20**, 1006-1020.

Tyson, P. D., and R. A. Preston-Whyte, 2000: *The Weather and Climate of Southern Africa.* Oxford University Press, Cape Town, 396 pp.

Wilby, R. L., and T. M. L. Wigley, 1997: Downscaling general circulation model output: a review of methods and limitations. *Progress in Physical Geography*, **21**, 530-548.

Wilks, D. S. 1995. *Statistical Methods in the Atmospheric Sciences*. Academic Press, San Diego, p. 467.

Wilks, D. S., 2001: Realizations of daily weather in forecast seasonal climate. *Journal of Hydrometeorology*, **3**, 195-207.

Zeng, X., M. Zhao, and R. E. Dickinson, 1998: Intercomparison of bulk aerodynamic algorithms for the computation of sea surface fluxes using TOGA COARE and TAO data. *Journal of Climate*, **11,** 2628-2644.